LA-UR-14-21983
Approved for public release; distribution is unlimited.

Title: Ranchero Armature Test LA-43-CT-2: PBXN-110 Explosive with no smoothing layer. Lower Slobovia, 6/13/13

Author(s): Marr-Lyon, Mark
Glover, Brian B.
Briggs, Matthew E.
Hare, Steven J.
Herrera, Dennis H.
Goforth, James H.
Rae, Philip
Watt, Robert G.
Rousculp, Christopher L.

Intended for: Referanceable shot documentation
Report

Issued: 2014-03-26

Ranchero Armature Test LA-43-CT-2: PBXN-110 Explosive with no smoothing layer. Lower Slobovia, 6/13/13

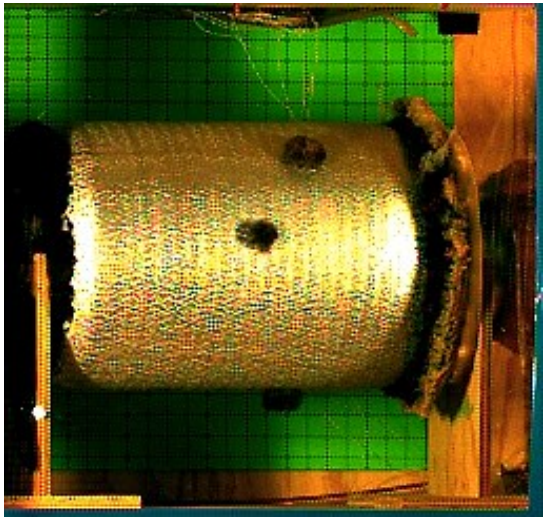

Mark Marr-Lyon, Brian Glover, Matt Briggs, Steve Hare, Dennis Herrera, Jim Goforth, Philip Rae, Bob Watt, Chris Rousculp

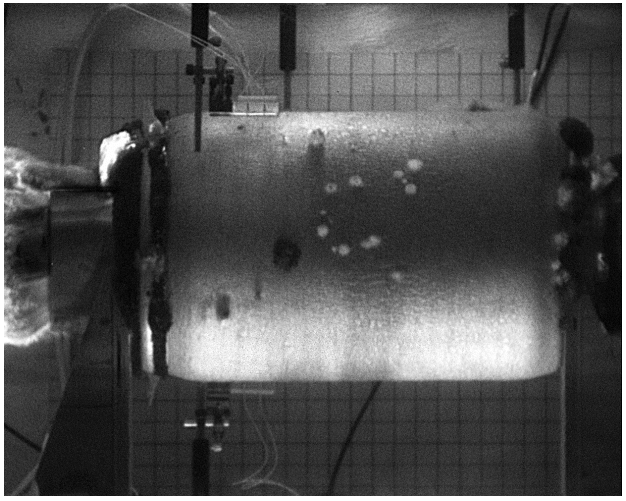

Ranchero Armature with smoother; 2X expansion. LA-43-CT-1; 1/11

Ranchero Armature without smoother; 2X expansion. LA-43-CT-2; 6/13

Abstract

This test, documented as LA-43-CT-2, was performed to verify calculations which indicate that the smoothing layer employed for Ranchero Armatures is not required when the slapper point spacing is 18 mm ("On the efficacy of an acrylic layer in the Ranchero armature," Bob Watt, published in "Ranchero Status Report" LA-14463). [Naming this test – CT-2 acknowledges the previous test performed during 1/11 as the initial test in the series, and we will refer to that test as LA-43-CT-1 in the future.] In addition, higher velocity is achieved when the volume occupied by the smoother is replaced by HE. Two framing cameras were used on the shot, and a 20 point PDV array was fielded to ascertain armature performance in specific conditions. The conclusions are that the armature is smooth enough, and the terminal velocity is increased from ~3.1 mm/µs to ~ 3.3 mm/µs. The armature tested had casting voids in the HE that were observed in pre-test inspections, and were expected to cause ruptures. (See Appendix 3 of the Ranchero Status Report.) Such "blowouts" were observed in all three locations identified in pre-shot inspection. In addition, ruptures occurred in locations having no pre-shot indication of a problem. These unpredicted blowouts have a difference in appearance from those typically seen. Further visual examination of the inspection radiographs do not reveal the cause, and that is a serious concern for future efforts with such castings. A path forward will include attempting to digitize the inspection x-rays for the charge tested, to see if the cause of the "new" ruptures can be found via computer enhancement. In addition, there are two additional armatures from the same casting lot, and these might also be tested to see if there is some problem with the HE or the armature material in this batch. For now, this plan is on hold, pending the outcome of tests and cost estimates related to using PBX-9501 in place of the PBXN-110. Casting issues would be eliminated in such configurations.

Ranchero Generators to-date, have employed the acrylic “smoothing layer” shown in the LA-43-2 cartoon below. LA-43-CT-2 diagnosed the performance of an armature using the same PBXN-110 castable explosive used in Ranchero generators without a smoothing layer

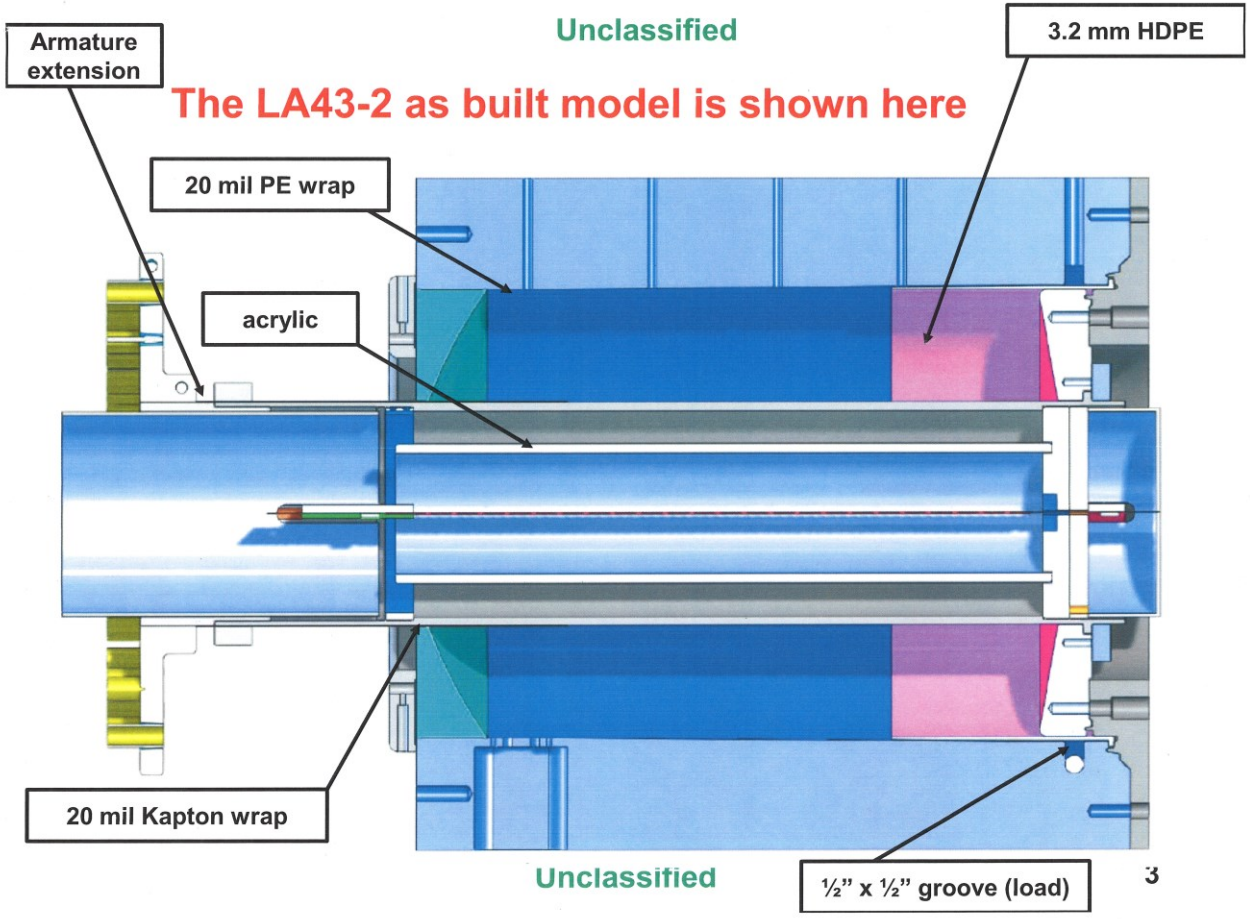

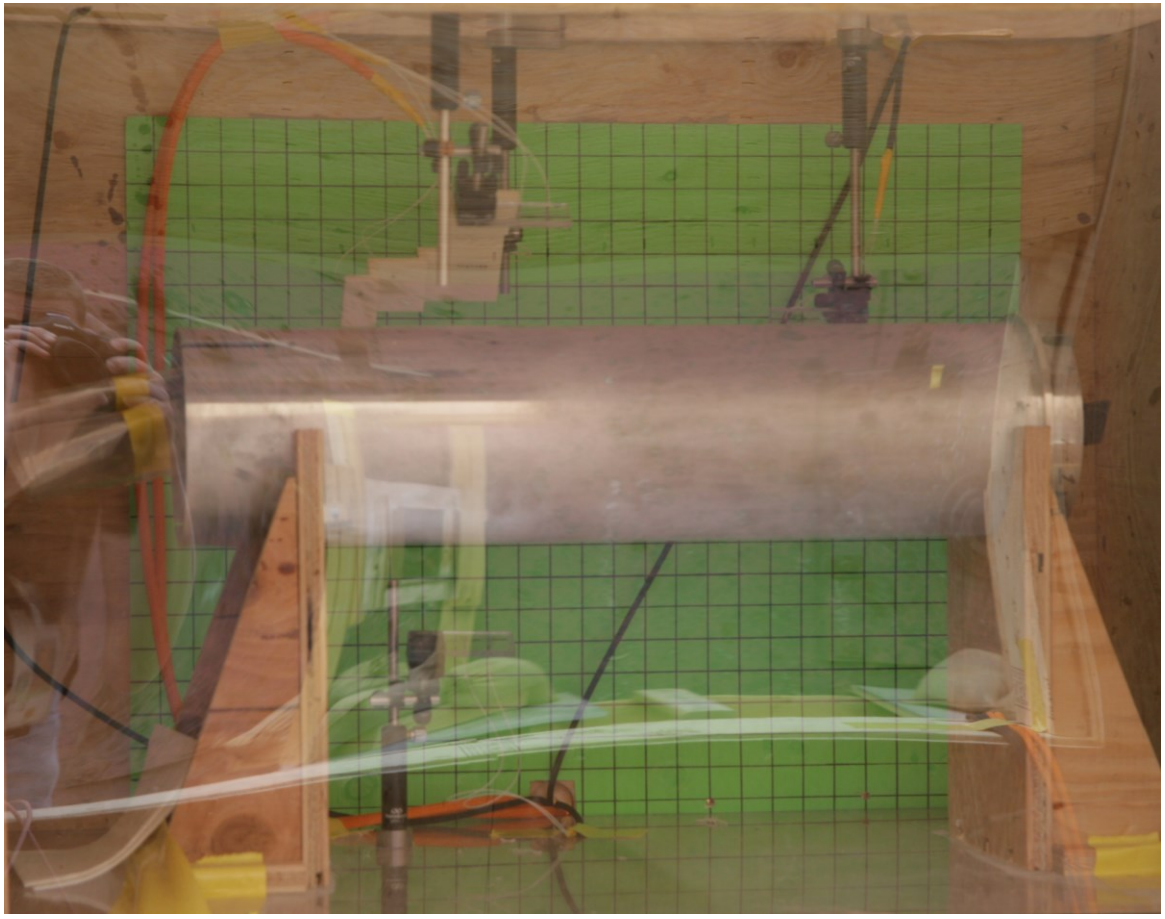

Ranchero Armature Pre-shot static image - 6/13/13. The enclosure is to contain the He atmosphere necessary to eliminate a shock on the leading edge of the armature which would obscure the armature surface. Glare on the front is off 1/16" Lexan sheet, which is used to prevent double images in the dynamic camera records. Holders for the PDV arrays are also seen hanging from the lid, and supported on the floor.

Purpose for Camera Test was:

1) Verify that smoothing layer was not needed with N-110 castings when point spacing was 18 mm (See Appendix 1 of Ranchero Status Report 2012 (LA-14463))
2) Field PDV arrays to answer a variety of pertinent questions

- Three armatures were available with N-110 cast into assemblies with 18 mm point spacing slappers and without smoothers
  - Part “one” had three bubbles
  - Parts “two and three” were bubble free
- It was decided to perform the camera test with part one.
  - This part would never be used on actual FCG test for fear of flux pocketing
  - The camera data would still verify that the smoother was or was not needed
  - PDV data would not be affected by bubbles
- PDV data were taken in four locations
  - One entire slapper to slapper space (7 probes)
  - Two locations on opposite sides of armature to measure lag at waist (parallel to cable)
  - Through two layers of 10 mil Kapton as was done on LA-43-2
  - “Transverse velocity” probes were also fielded as an add-on experiment

PDV Data

Matt Briggs and Steve Hare

Imbedded files give a movie on slide 7 (with Quicktime), and an Excell spread sheet of data on slide 13.

Video of probe array illumination starts at approximate initial cylinder location.

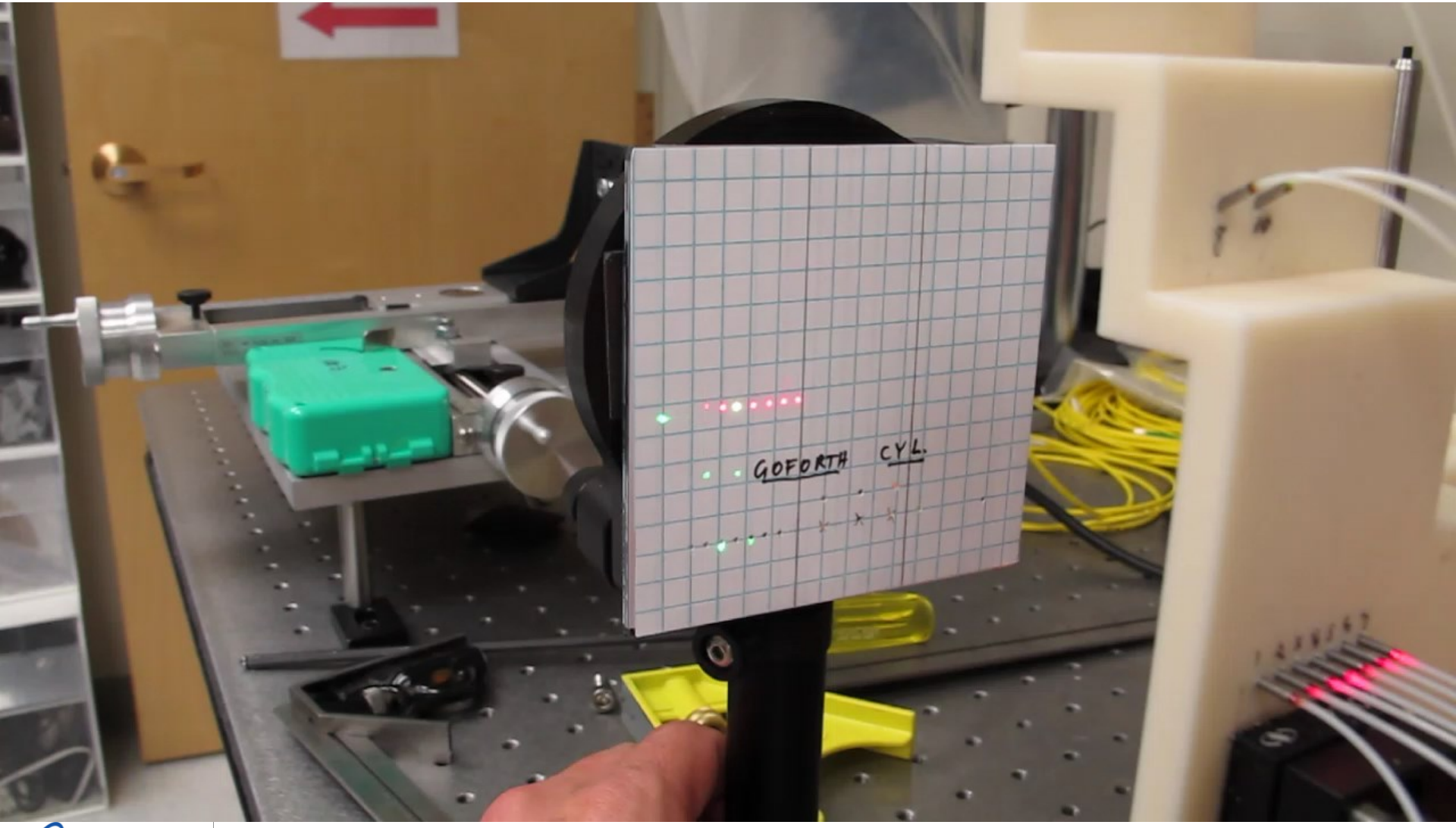

PDV probes arrayed to test armature performance by measuring variations between 2 detonators (1—7), and around the cylinder (14—17, 90° above and below 1—7), and obliquely to test for anomalies in non-radial PDV signals (8—13).

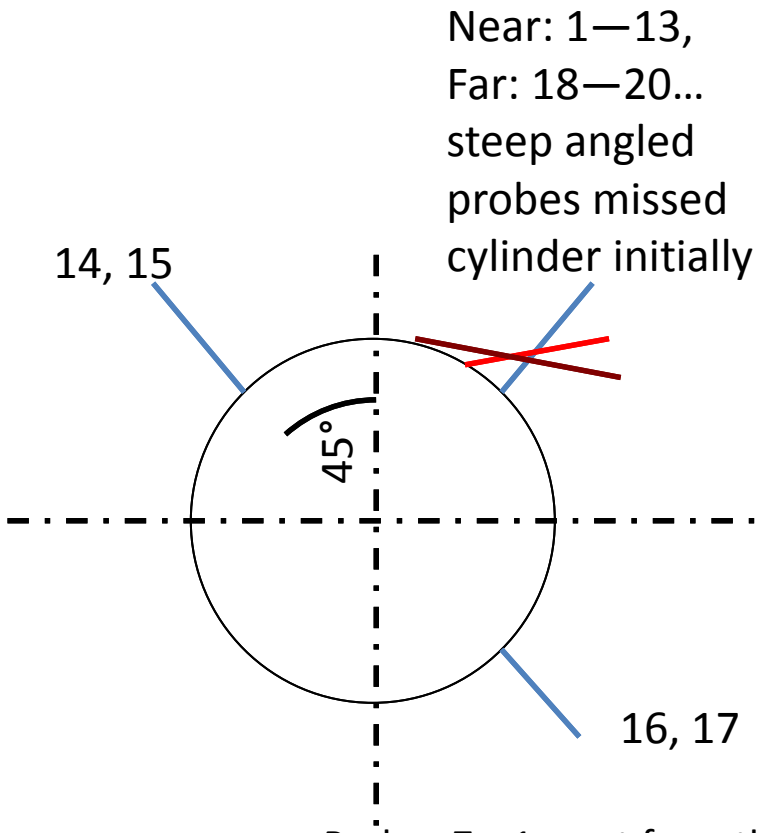

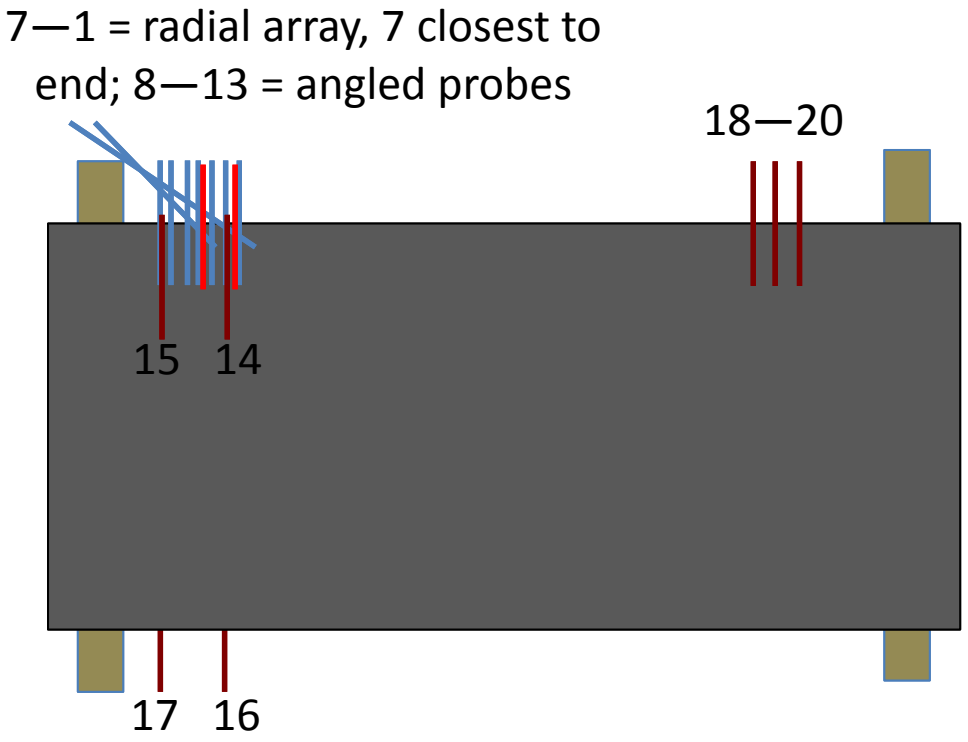

Probes 7—1 went from the cabled end of the cylinder, starting at 218 mm, and spaced 3.475 mm ± 0.2 mm, ending at 238.85 mm.
Probes 8—13 were angled. These were an add-on experiment, and analysis will be performed as time allows.
Probes 15 & 14, and 17 & 16 were at 218 and 236 mm from the end, with 15 & 14 above the cylinder and 17 & 16 below.

PDV design for Ranchero Cylinders – the 13 probe array

This array had 7 probes to measure the smoothness of shock break-out, and 6 probes at angles to look for a recently discovered effect of surface strain on PDV measurements.

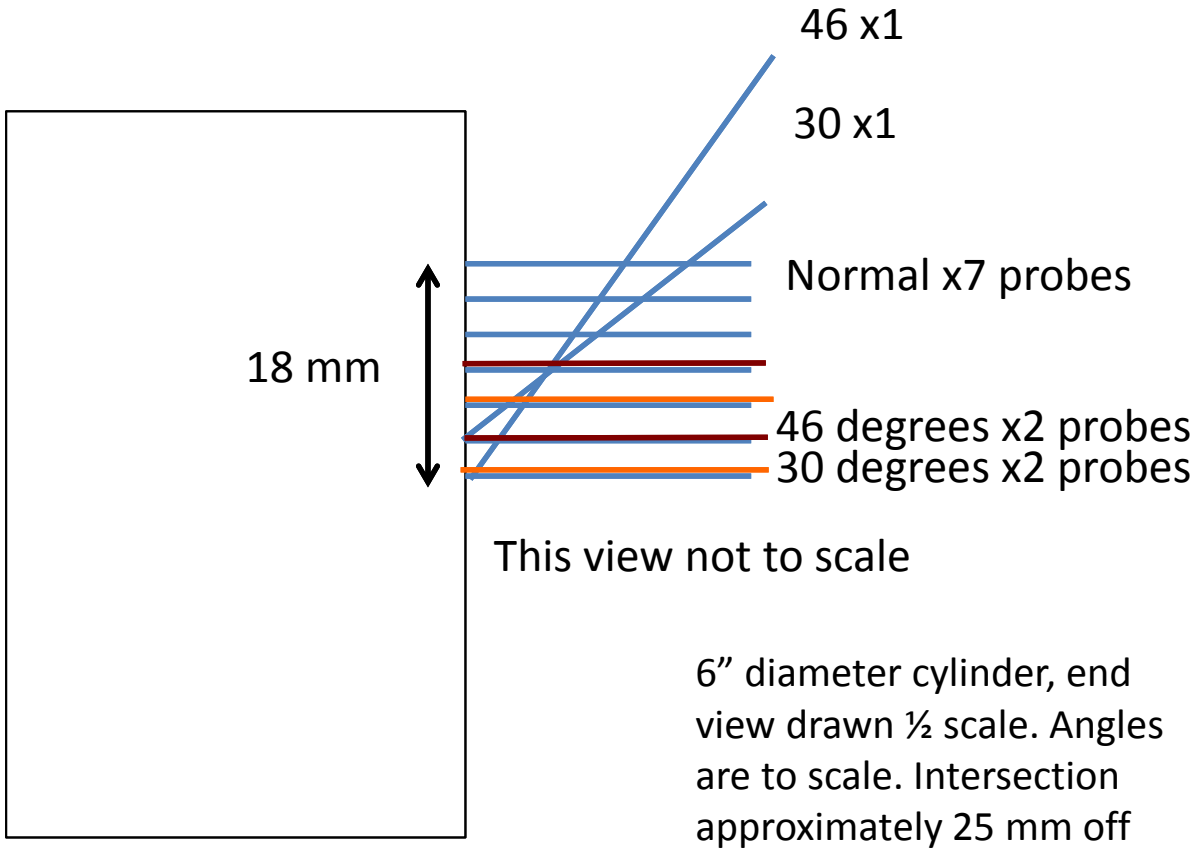

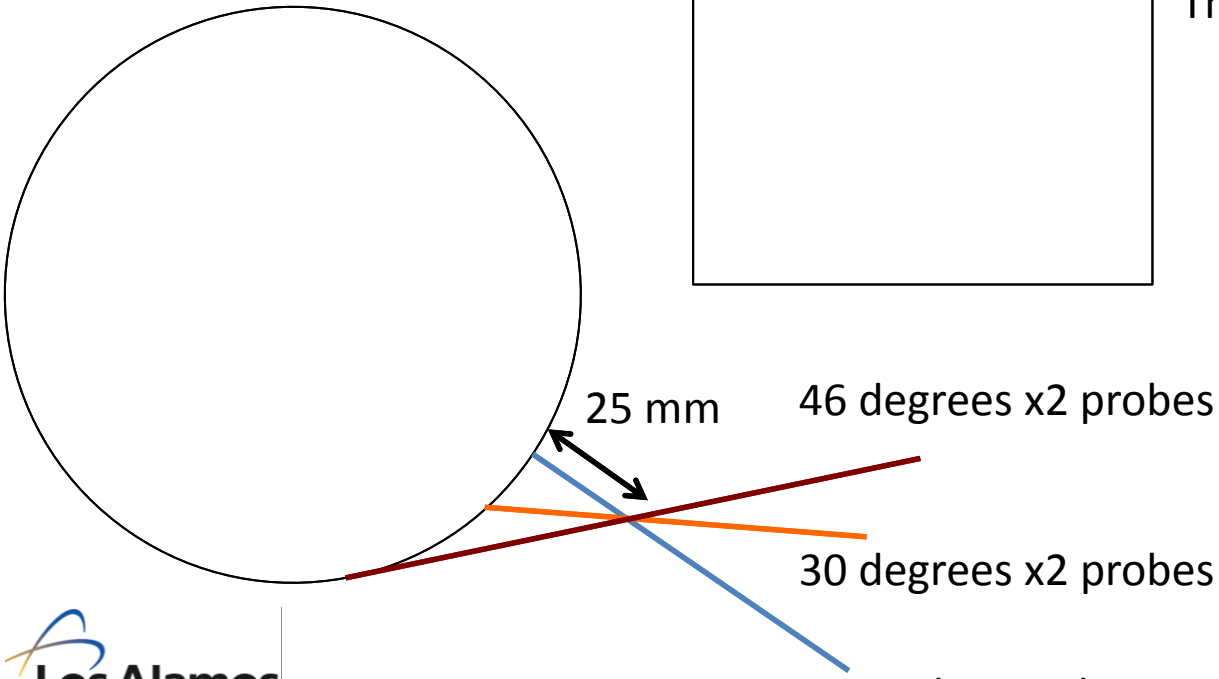

6” diameter cylinder, end view drawn ½ scale. Angles are to scale. Intersection approximately 25 mm off surface. Two probes were added to the cluster of 5 fielded on LA-43-CT1, so the stack at right would have 7 probes evenly spaced over 18 mm

Details of the 13 probe array: 100 mm to foci, which were at the crossing of angled and normal probes, 25 mm from surface. Inset is view from the back.

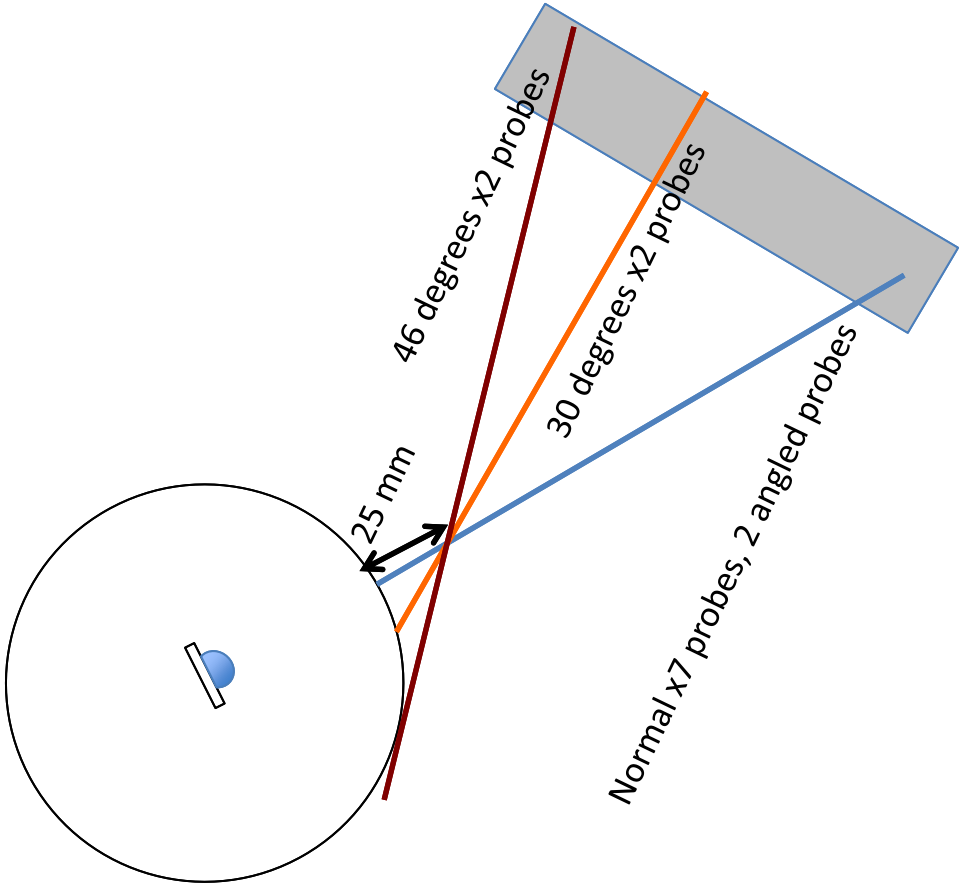

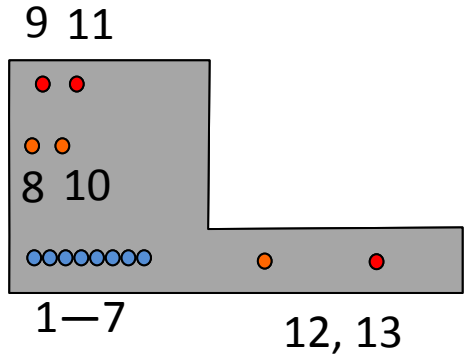

Probe array build showing the beams at the crossing plane. The 6 angled probes (8—13 are overlapping 6 of the 7 normal probes (1—7.)

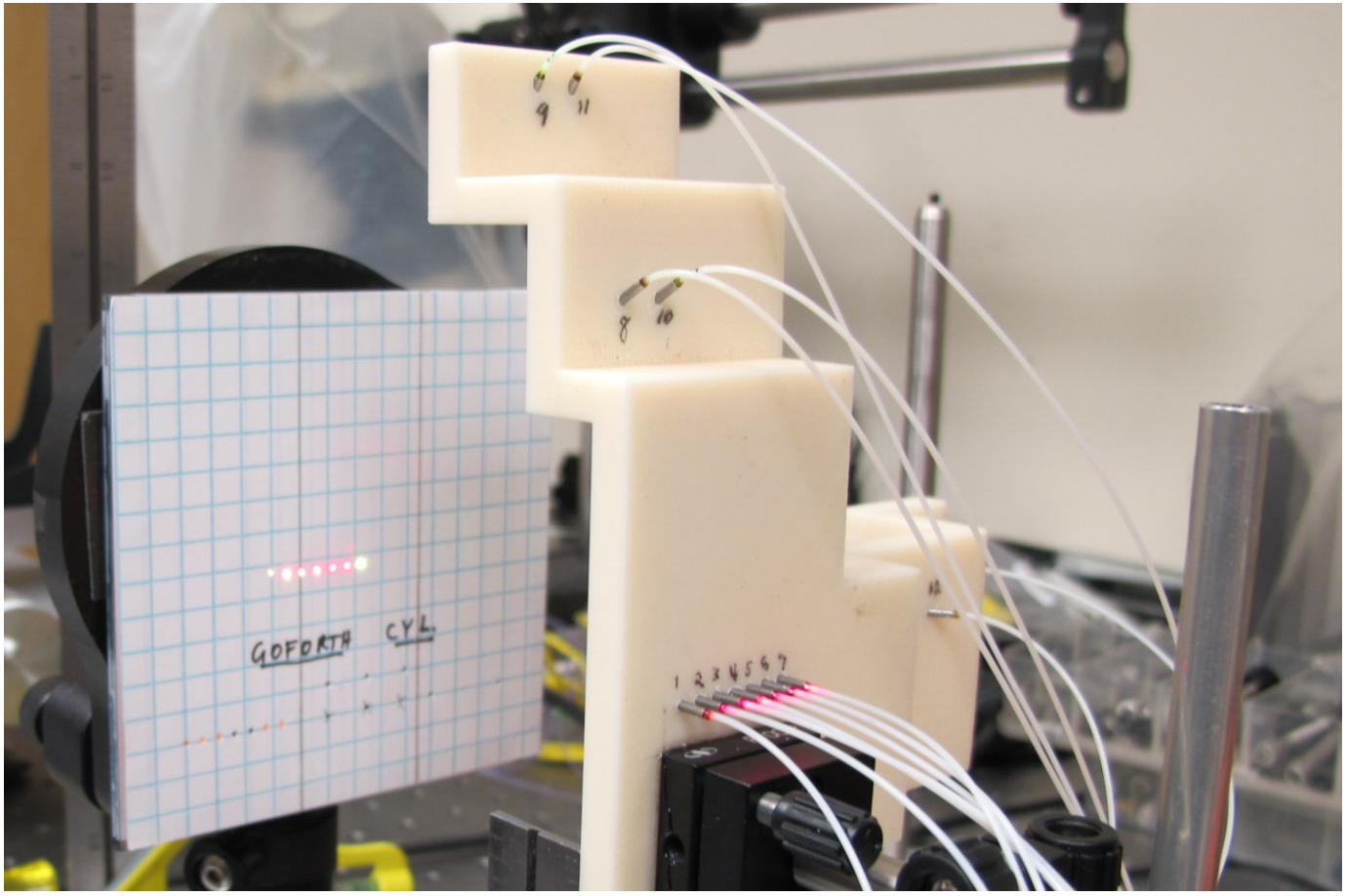

We used an optical pulse generator and measured cable delays to correct the PDV channels timing relative to each other to < 1 ns, and to the shot trigger to 10 ns.

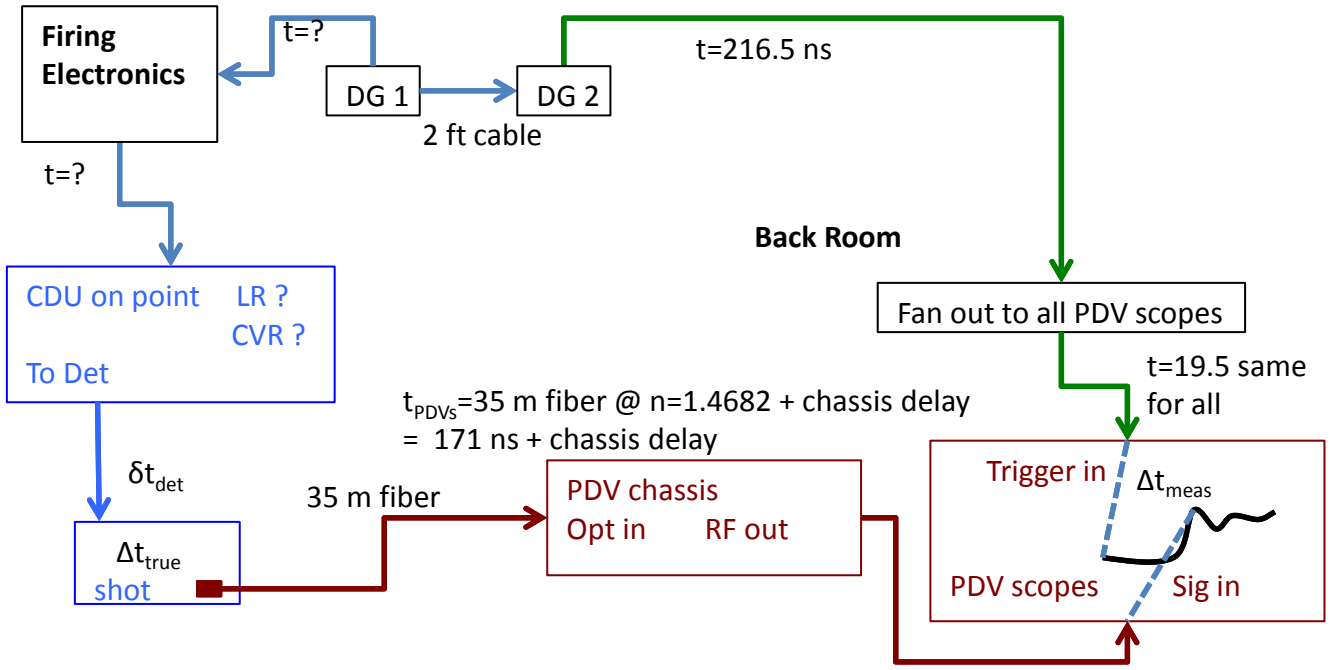

Lump unknown times into δt_{det}:

Δt_{true} + .171 + chassis delay − Δt_{meas} – .0195 – .2165 + δt_{det} = 0 in us

$\Delta t_{true} = \Delta t_{meas}$ + .0195 + .2165 − .171 – chassis delay – δt_{det}

$\Delta t_{true} = \Delta t_{meas}$ + .065 – chassis delay – δt_{det}

Timing correction to shot trigger table

Probe	SOM-uncorr (us)	uncertainty	Scope bandwidth, sample rate	SOM-corr	position on Armature		meas ch delay	tester offset	final ch delay
1	17.667	.2 ns	8 GHz, 20 GS/s	17.68344	238.85	Mace rack	0.03926	0.0093	0.04856
2	17.667	0.2	8 GHz, 20 GS/s	17.68534	235.375	Mace rack	0.03736	0.0093	0.04666
3	17.666	0.2	8 GHz, 20 GS/s	17.68464	231.9	Mace rack	0.03706	0.0093	0.04636
4	17.6665	0.2	8 GHz, 20 GS/s	17.68454	228.425	Mace rack	0.03766	0.0093	0.04696
5	17.6535	0.2	16 GHz, 50 GS/s	17.6826	224.95	Briggs rack	0.0217	0.0142	0.0359
6	17.6515	0.2	16 GHz, 50 GS/s	17.6803	221.475	Briggs rack	0.022	0.0142	0.0362
7	17.6517	0.2	16 GHz, 50 GS/s	17.67894	218	Briggs rack	0.02356	0.0142	0.03776
8	17.6221	0.1	16 GHz, 50 GS/s angled*	17.63199	238.85	Agilent rack	0.04581	0.0093	0.05511
9	18.25	50	16 GHz, 50 GS/s angled*	18.26149	235.375	Agilent rack	0.04421	0.0093	0.05351
10	17.6215	0.1	16 GHz, 50 GS/s angled*	17.63159	231.9	Agilent rack	0.04561	0.0093	0.05491
11	18.3	50	16 GHz, 50 GS/s angled*	18.31039	228.425	Agilent rack	0.04531	0.0093	0.05461
12	17.6574	0.1	8 GHz, 25 GS/s angled*	17.6831	232.4	hull rack	0.03	0.0093	0.0393
13	18.7	500	8 GHz, 25 GS/s, angled*	18.7257	246.8	hull rack	0.03	0.0093	0.0393
14	18.0268	0.1	8 GHz, 25 GS/s	18.0518	236	hull rack	0.0307	0.0093	0.04
15	18.0175	0.1	8 GHz, 25 GS/s	18.0426	218	hull rack	0.0306	0.0093	0.0399
16	18.0106	0.1	8 GHz, 25 GS/s	18.03988	236	Briggs rack	0.02152	0.0142	0.03572
17	18.012	3	16 GHz, 50 GS/s, weak signal	18.04068	218	Briggs rack	0.02212	0.0142	0.03632
18	17.6125	0.2	16 GHz, 50 GS/s	17.64158		Briggs rack	0.02172	0.0142	0.03592
19	17.6161	0.2	16 GHz, 50 GS/s	17.64586		Briggs rack	0.02104	0.0142	0.03524
20	17.6221	0.2	16 GHz, 50 GS/s	17.65154		Briggs rack	0.02136	0.0142	0.03556

Trig delay DG back to fanout in optics room = 216.5 ns; 19.5 ns fan-out to scope

Fiber delays 30 + 5 m @ 1.4682 = 171 ns

time corr = trig delay - fiber delay - final ch delay

*Angled probes start of motion had very weak signal, and 9 & 11 missed the surface at the start, and are therefore expected to be very late

PDV signals at start of motion as recorded on the oscilloscopes for the 7 probe array show jump-off with < 1ns resolution. They were in a line spaced evenly over 20.8 mm; 1—4 (up from bottom) were on one PDV chassis, 5-7 on a 2nd; These oscilloscope traces are not time corrected. The shift in the bottom 4 is due to a chassis to chassis difference. The starts of motion shown in later slides use time-corrected jump-offs taken directly from these oscilloscope records.

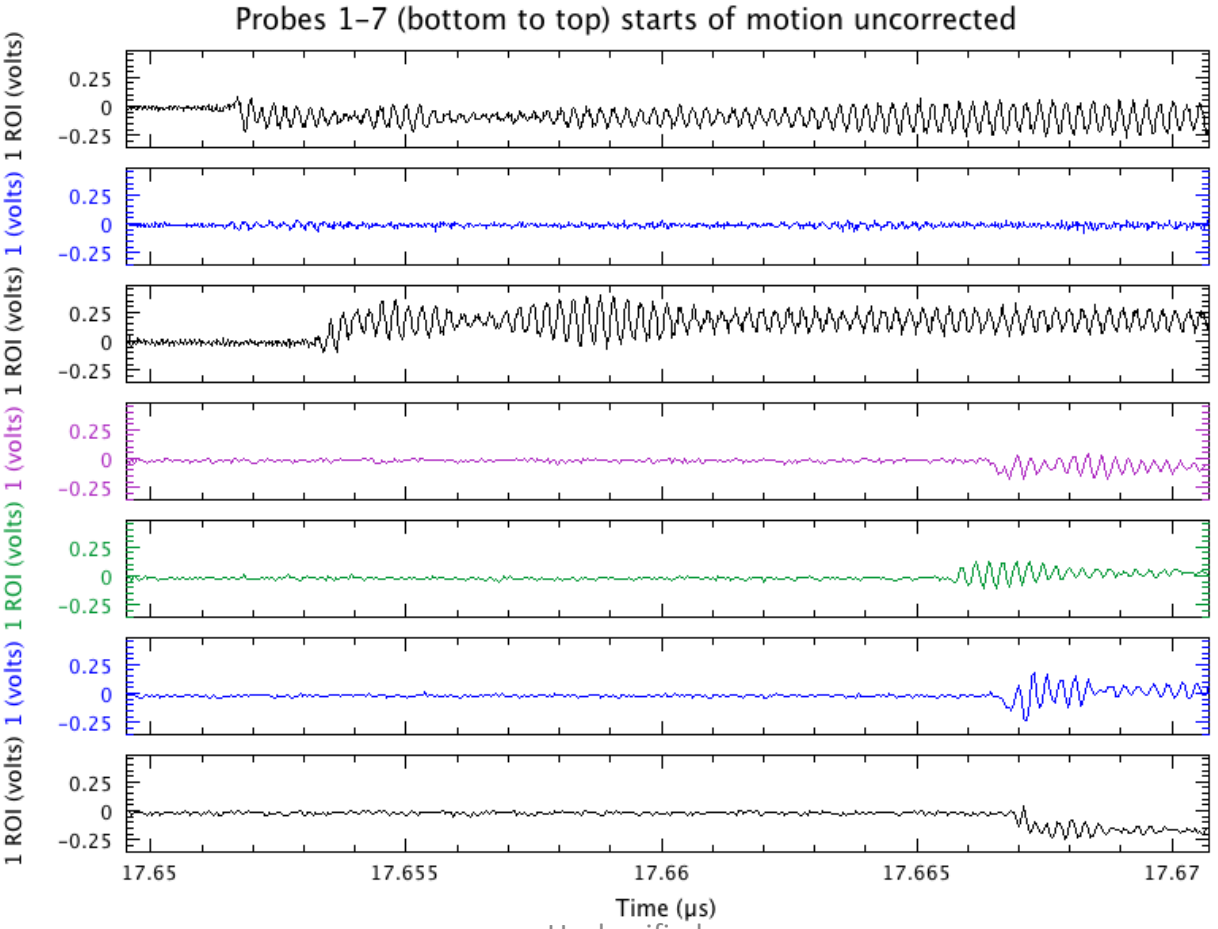

Time corrected results: 1—7 were within 7 ns of each other, the 90° probes came in ~350 ns later than 1—7. Starts of motion corrected to shot trigger plotted vs. position in mm along tube, 0 distance = det cable side of tube; correction is missing a common delay of the time of the firing cables and detonator function time. Relative timing ±1 ns.

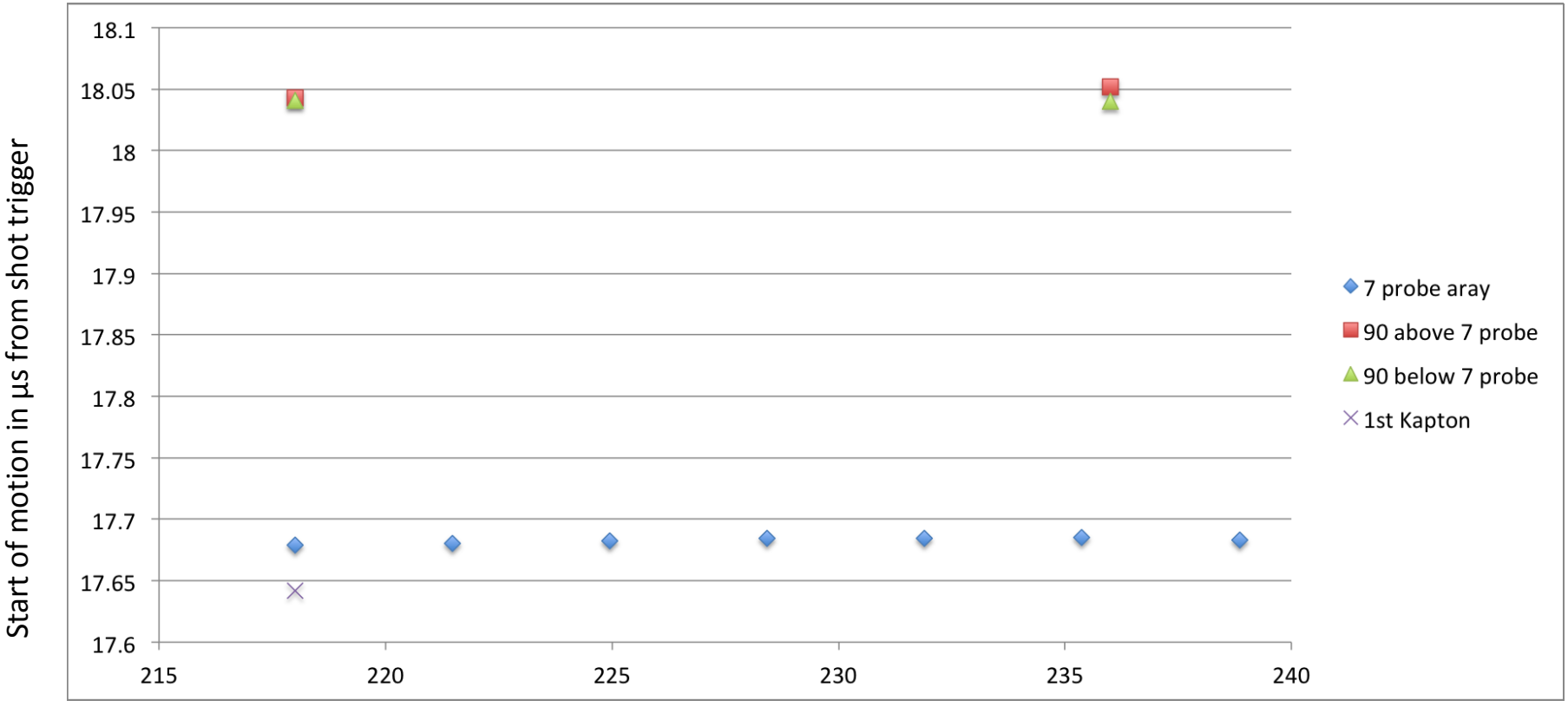

The spread in jump-off times between 2 detonators was just over 6 ns. Starts of motion corrected to shot trigger vs. position in mm along tube, 0 = det cable side of tube; uncertainty ~ marker size, errors ± 1 ns.

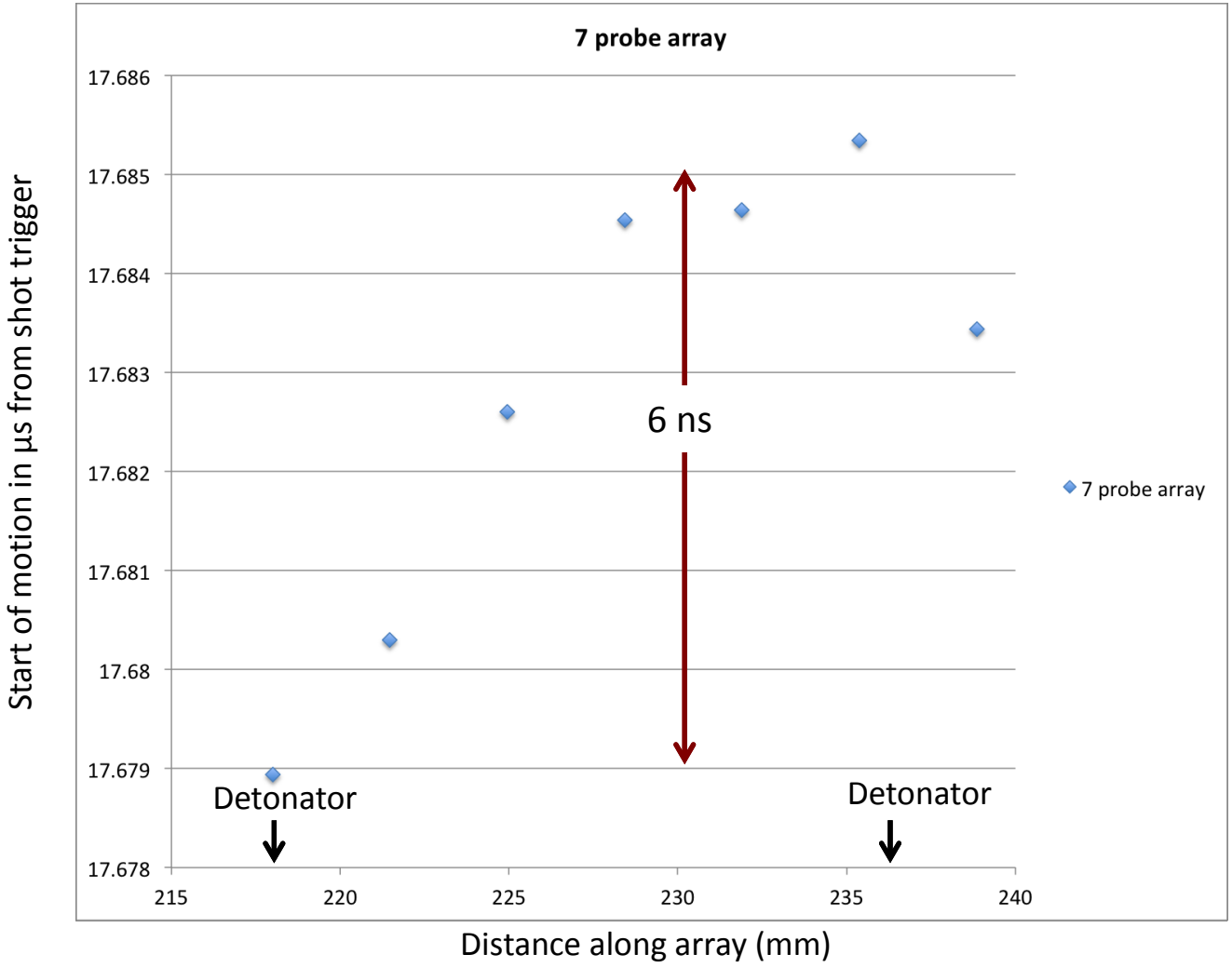

There is no obvious correlation between the pattern in the jump off speeds (lower) and the jump off times (upper); error bars on jump off speeds ~ size of variation

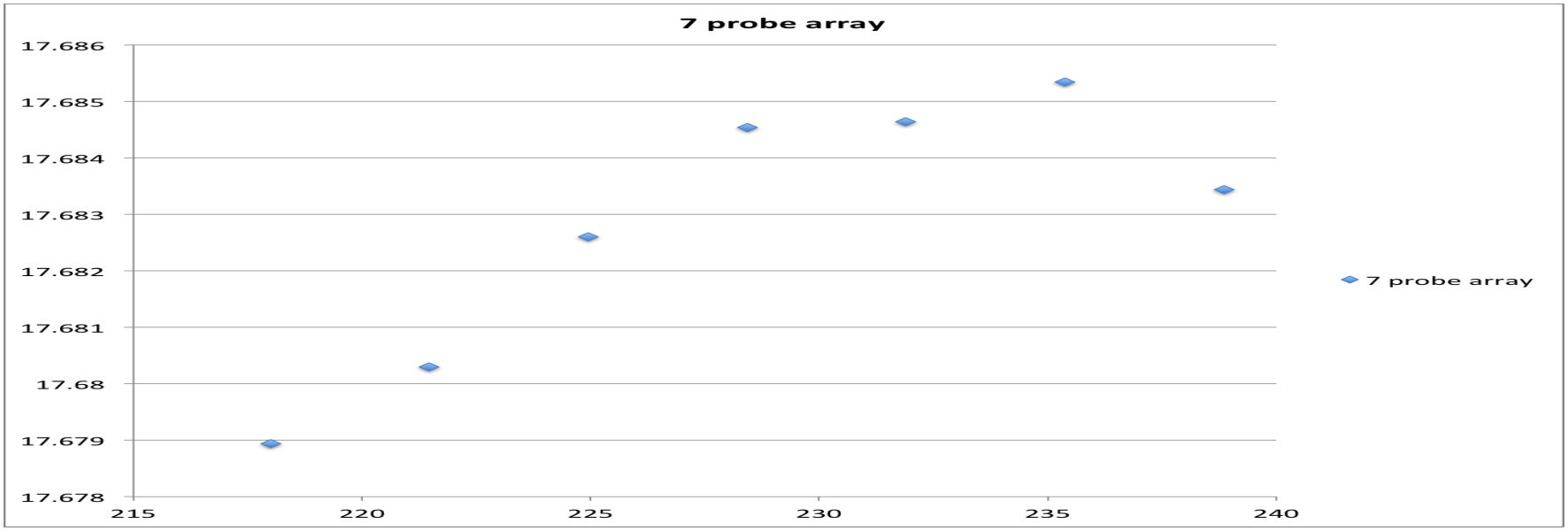

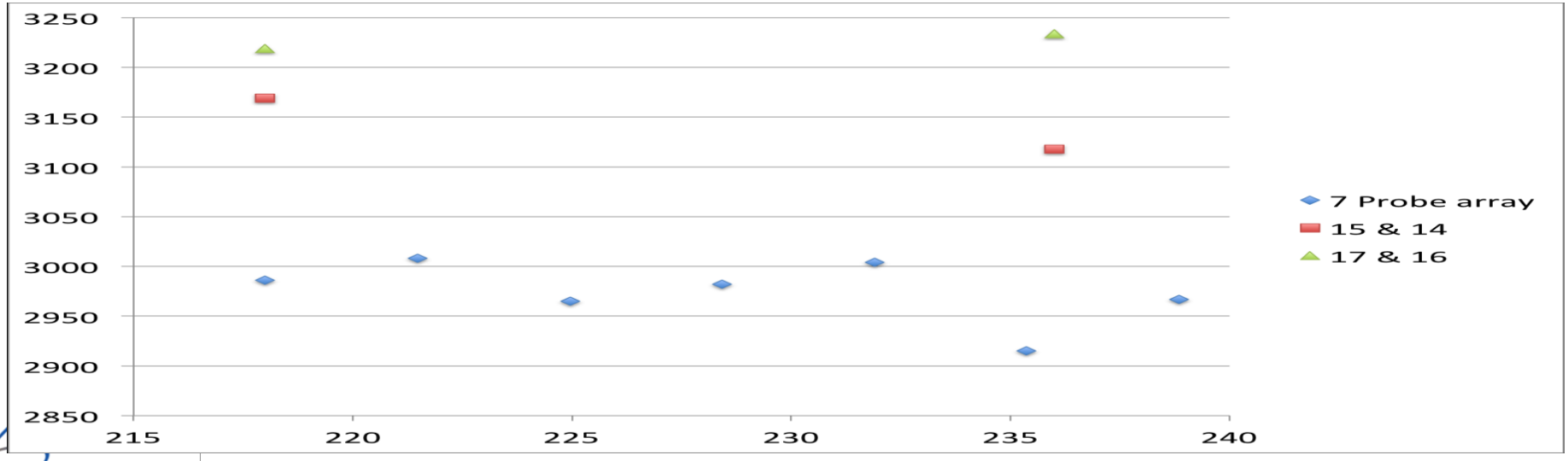

Jump-off speeds were higher for the points that jumped off later

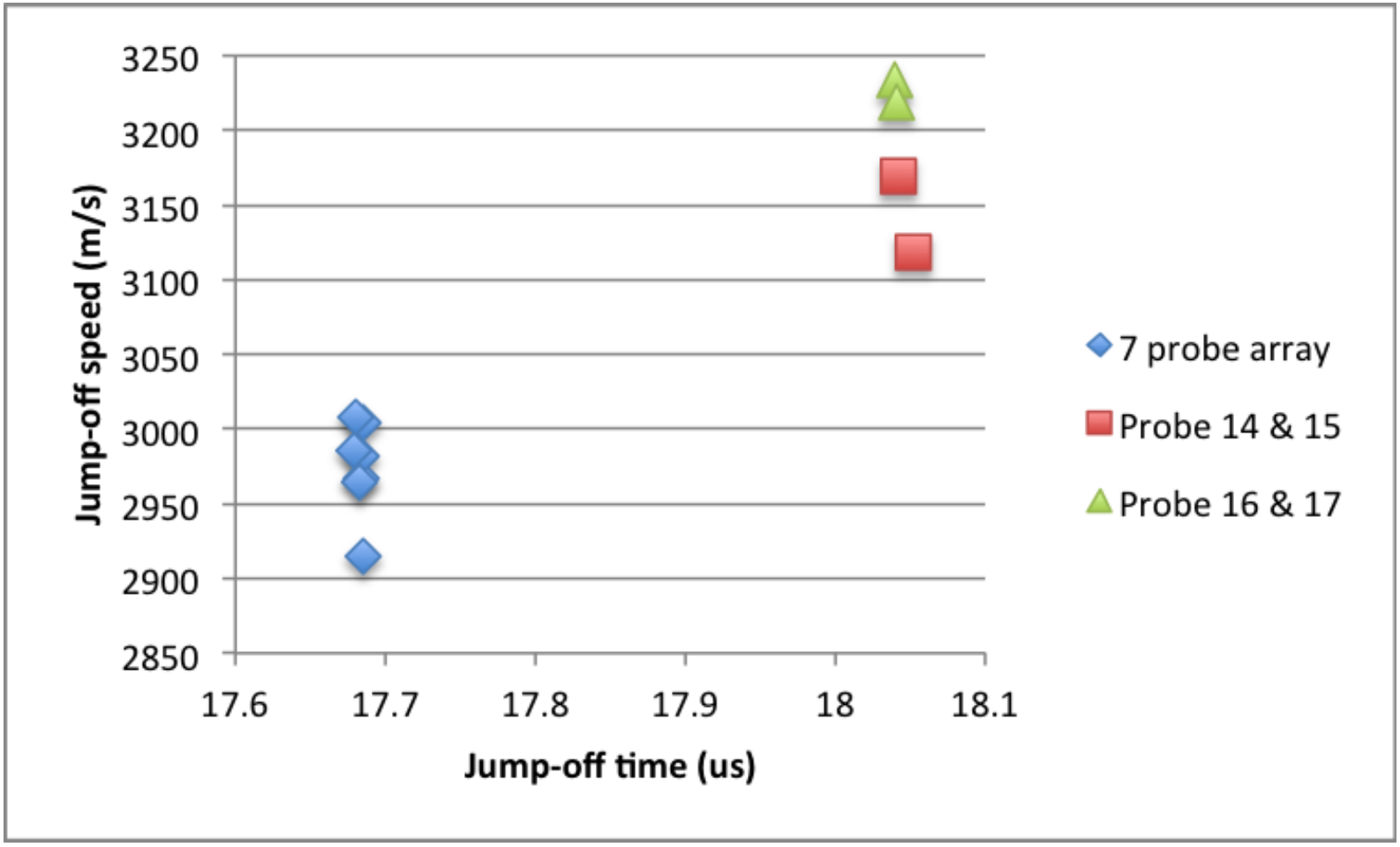

Perhaps the re-shock time pattern lines up with the detonators

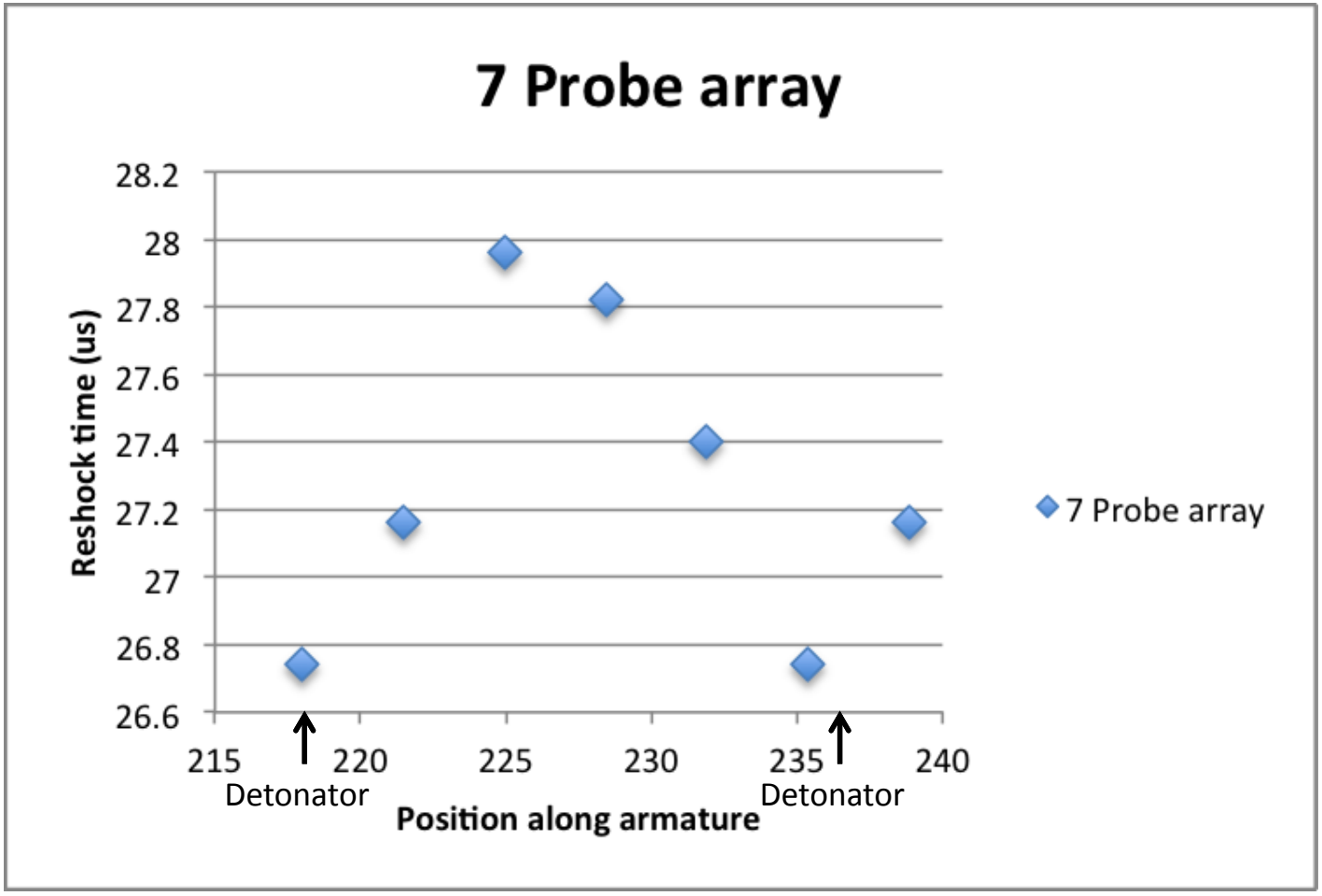

An example spectrogram analysis of a radial probe. Black is the speed extracted from the spectrogram (the red box constrains the extraction algorithm). The inset shows about 50 ns at the start of motion, with the extraction and oscilloscope record superimposed on the spectrogram. There are a few oscillations within each spectrogram bin, which is why the start of motion can be obtained with higher resolution directly from the oscilloscope record.

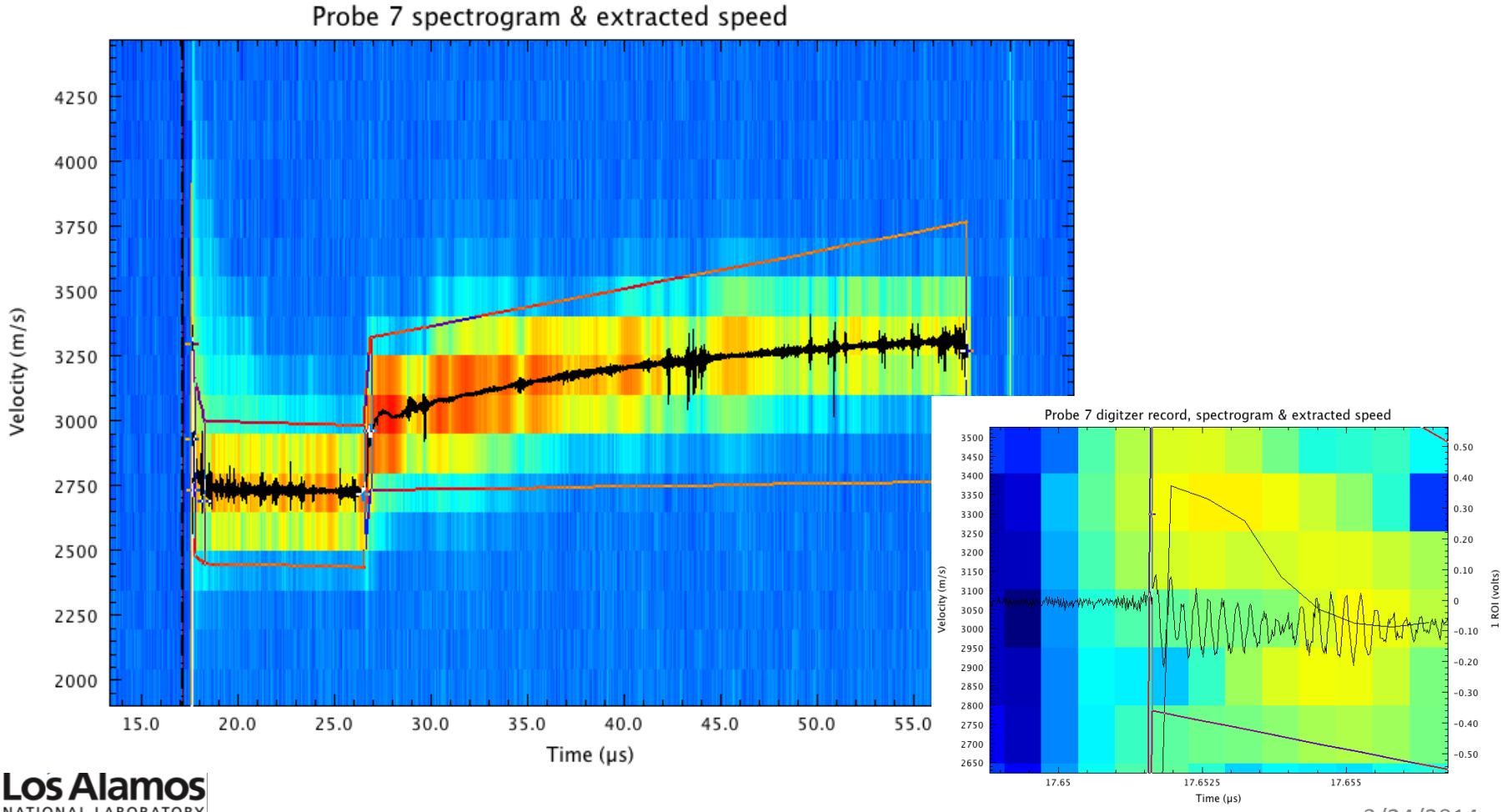

The three Kapton probes. Three velocities are seen. There are two layers of Kapton, and the armature underneath it. Best interpretation is that return signals were good off both layers of Kapton and there was "ejecta" off the surface of the outer layer. The Aluminum armature does not return a signal, and does not catch up to the Kapton before the end of the record.

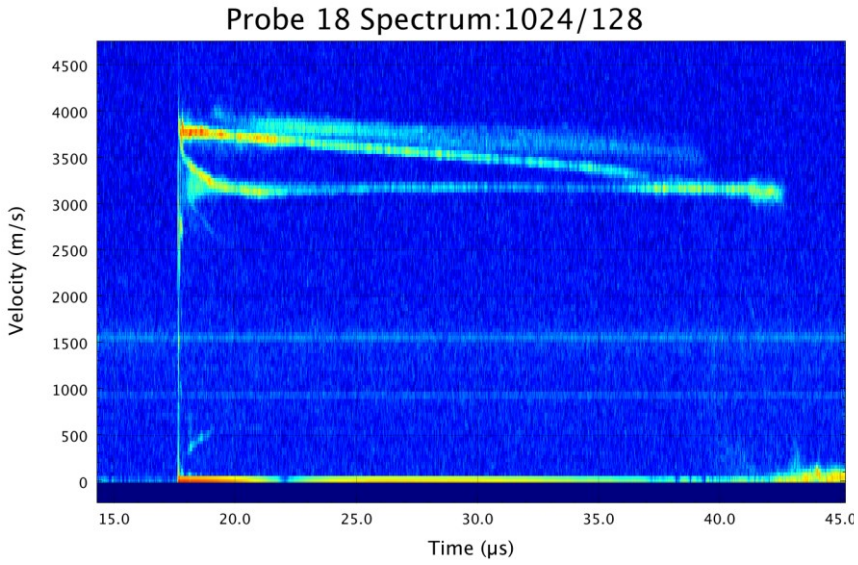

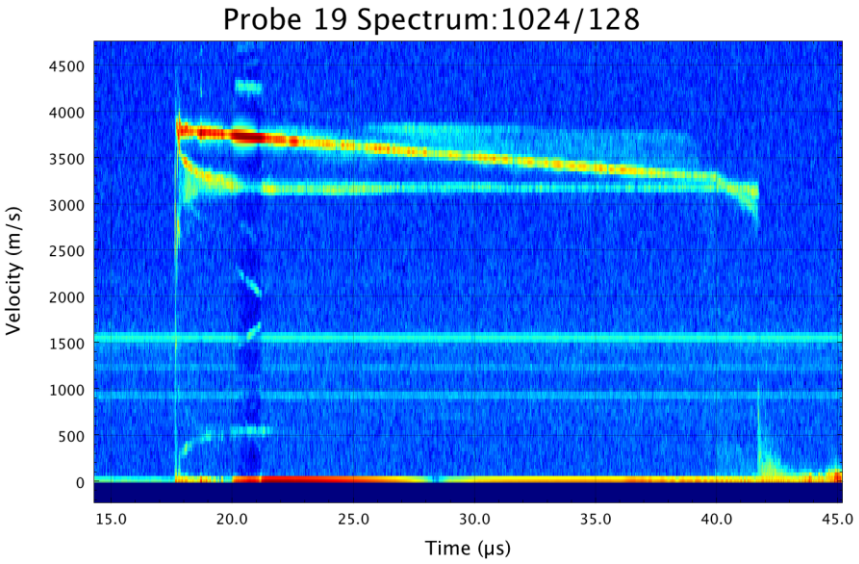

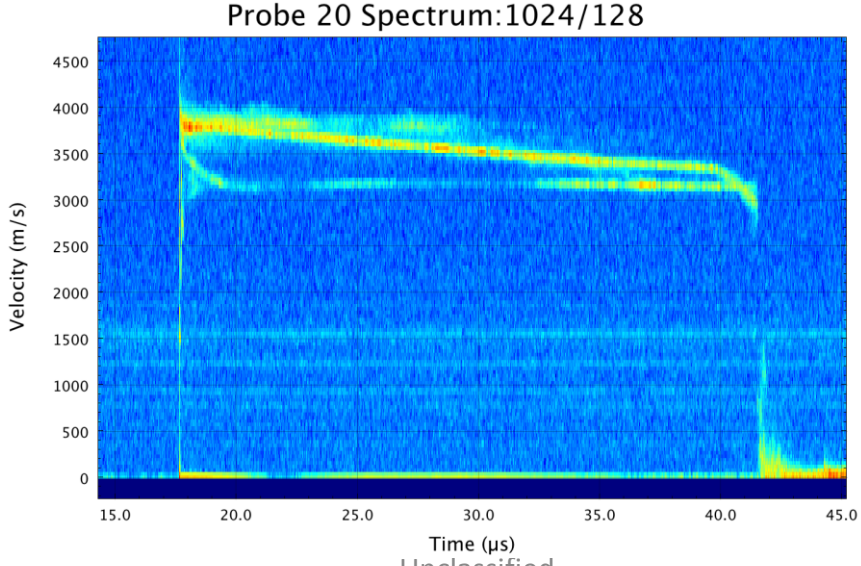

Rich structure for the Kapton probes at early times, interpretation uncertain (black is the oscilloscope record superimposed.) Insets are the first 100 & 25 ns.

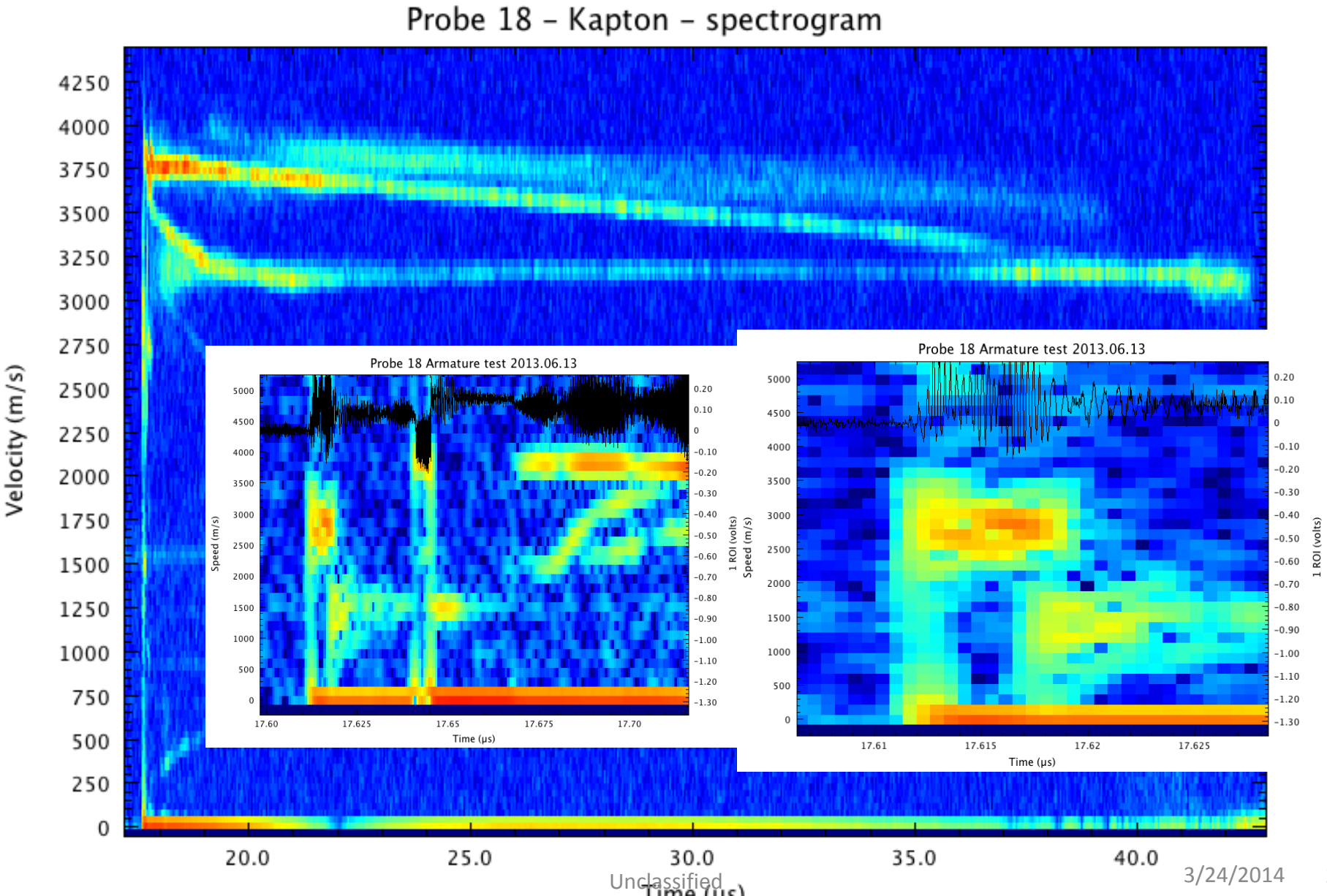

On LA-43-2, PDV data were taken of the armature, but looking through the input insulator Kapton; 2 wraps of 10 mil. The data taken on this test do not match, and there is much speculation, but no concrete conclusions

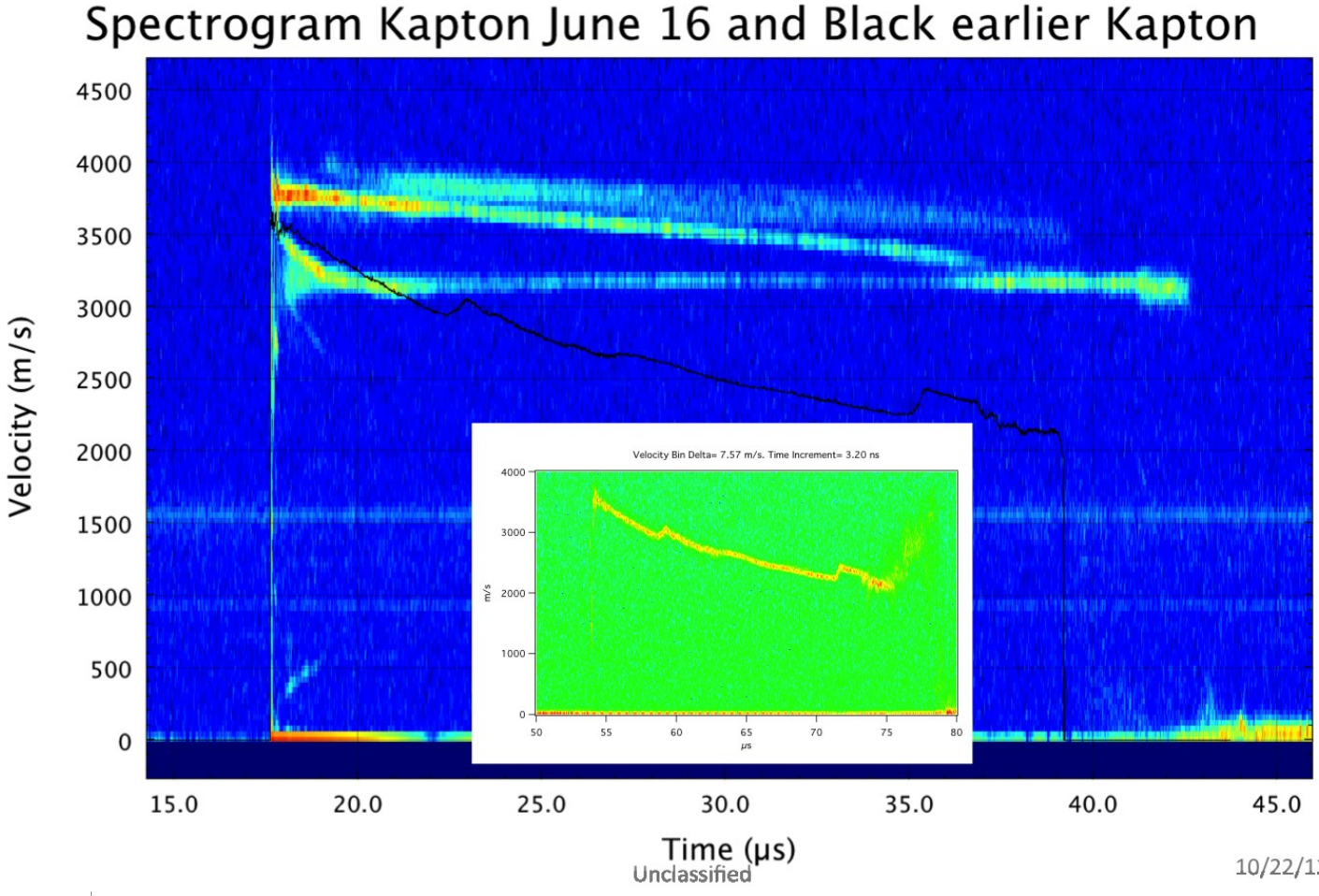

Comments and speculation about the two tests

- LA-43-2 gives a single velocity curve, shown here, which consists of a jump-off, then a gradua decay with some apparent recollection steps.
- LA-43-CT-2 gave three curves.
  - Ejecta off Kapton and two Kapton layers?
  - Two layers of Kapton and the Armature?
    - The armature, then, shows no spall and recollection
    - The armature never gets up to the velocity seen on other probes
- Analysis of data on LA-43-2 would have seen ejecta off the Kapton.
- There is more HE on this test because the smoother is left out.
- The surface of the Kapton was roughed with Scotchbrite on CT-2 but not 43-2.
- CT-2 had two patches of Kapton taped to the surface, but 43-2 had two wraps.

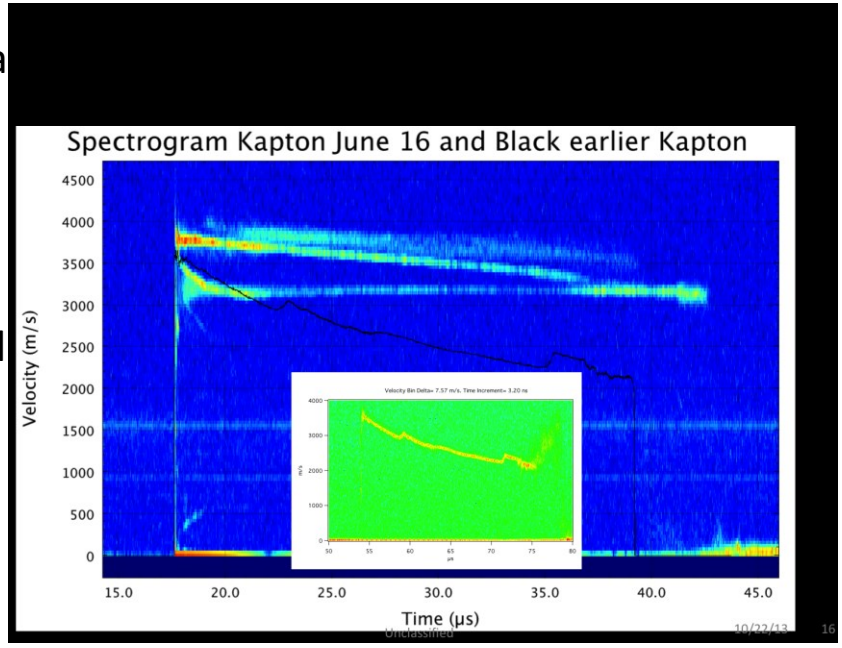

- The armature never caught up to the Kapton on 43-2.

There were ejecta present; speeds and contours suggest three observations.

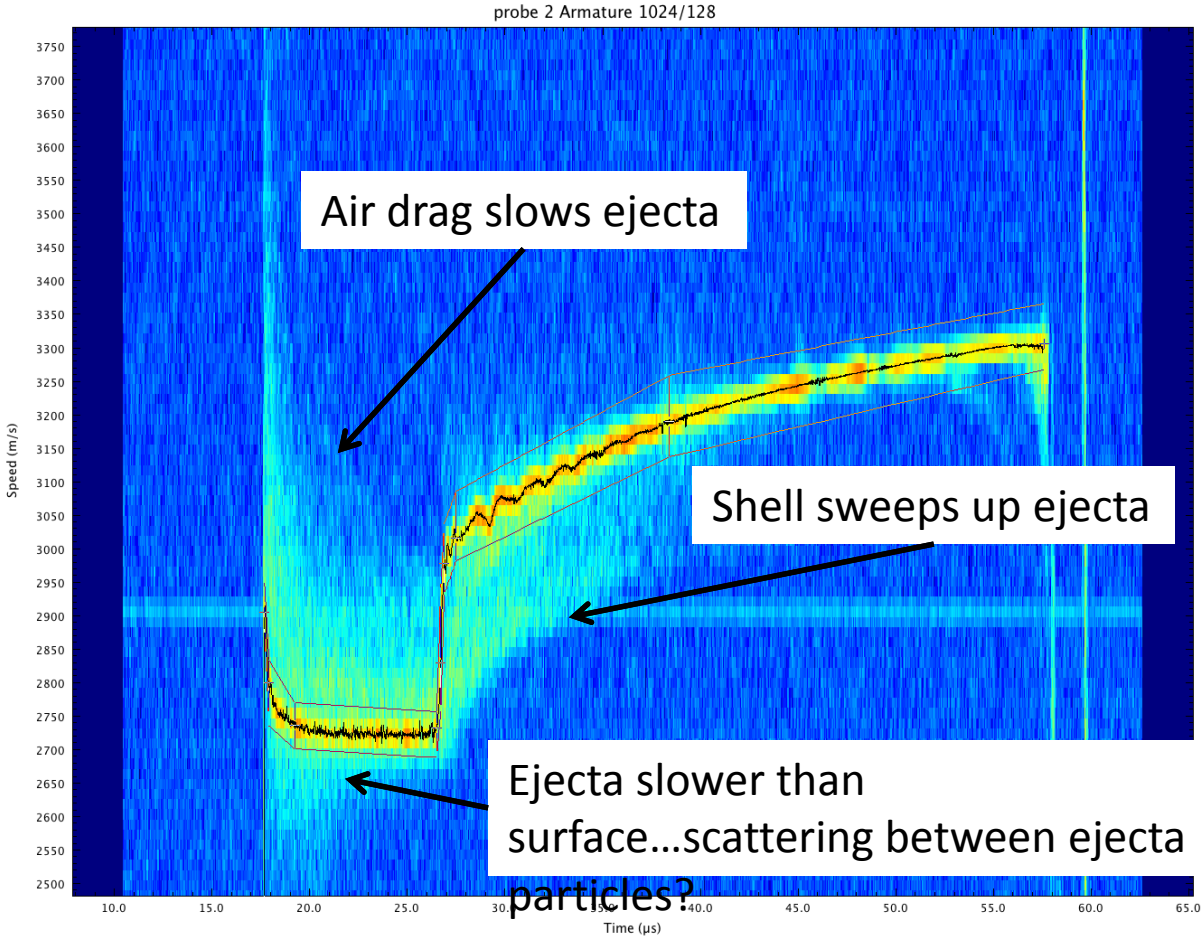

The ejecta complicates the analysis; my results were done as in the lower right plot, excluding the ejecta

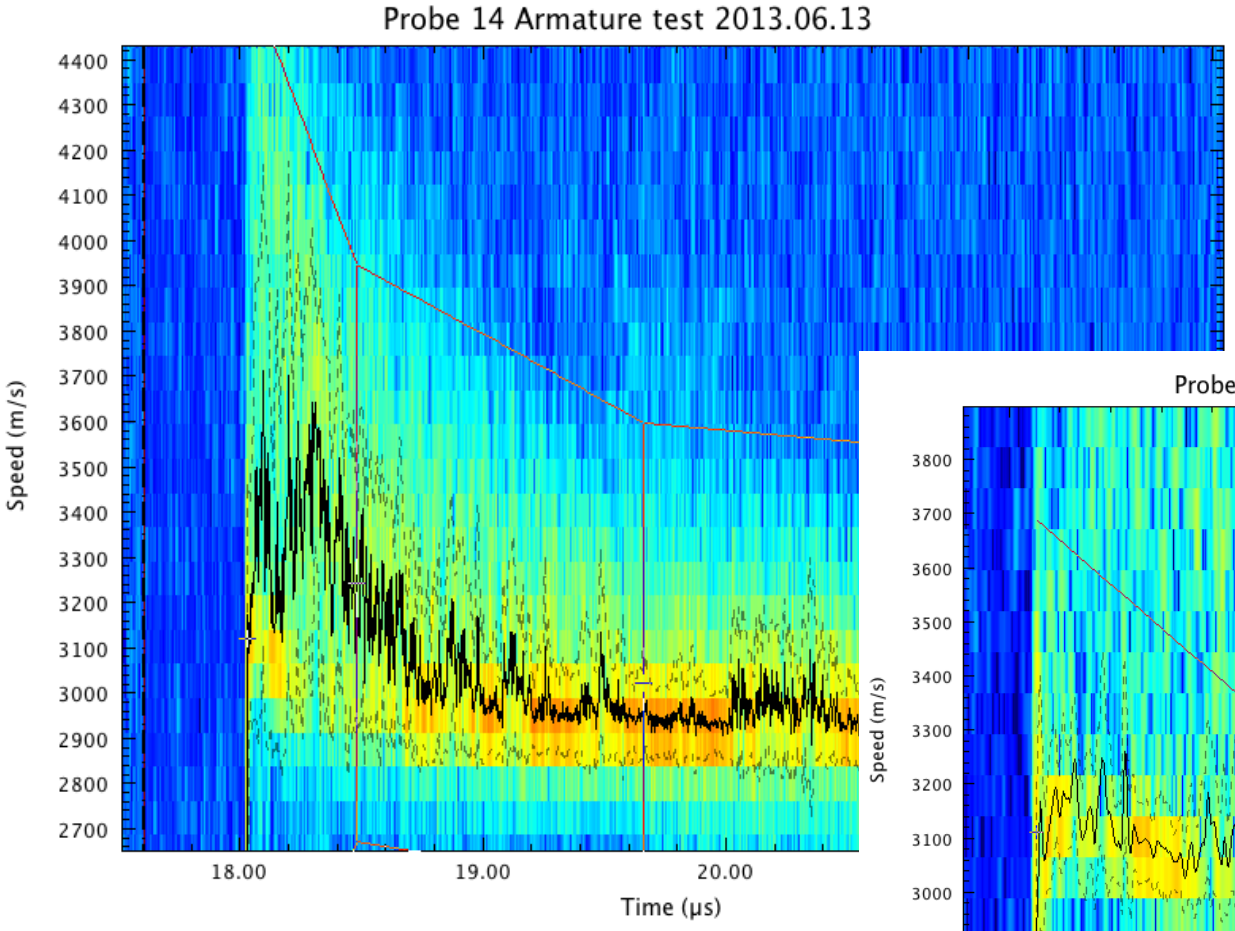

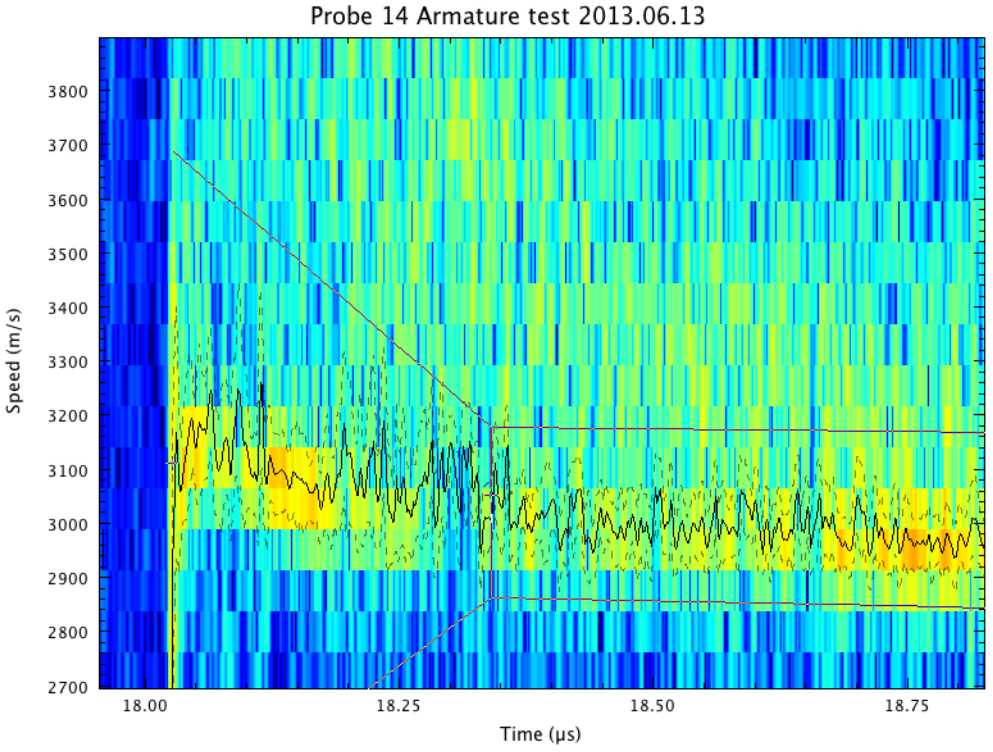

Some points seemed to have a brief velocity spike at start of motion (lower right), some did not (upper left)

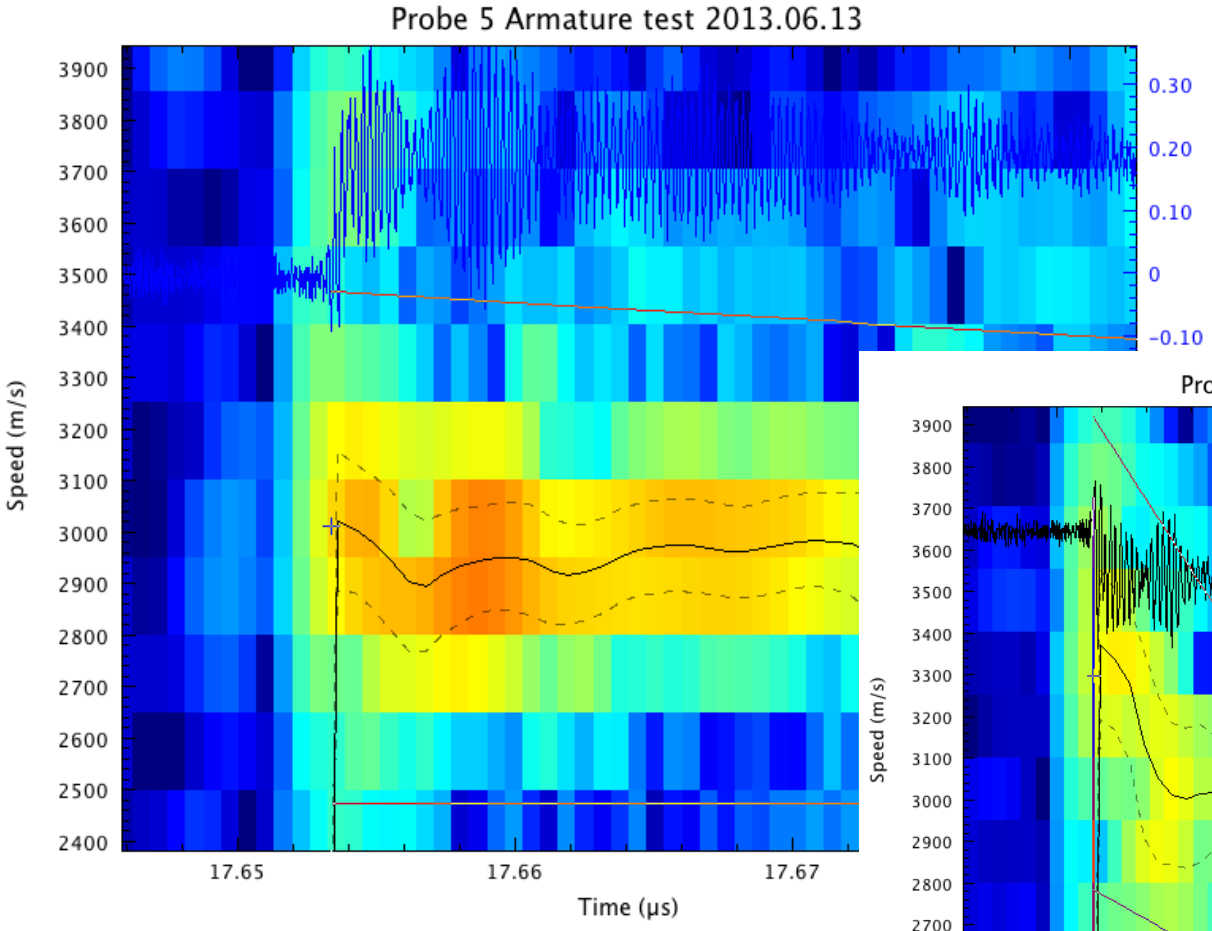

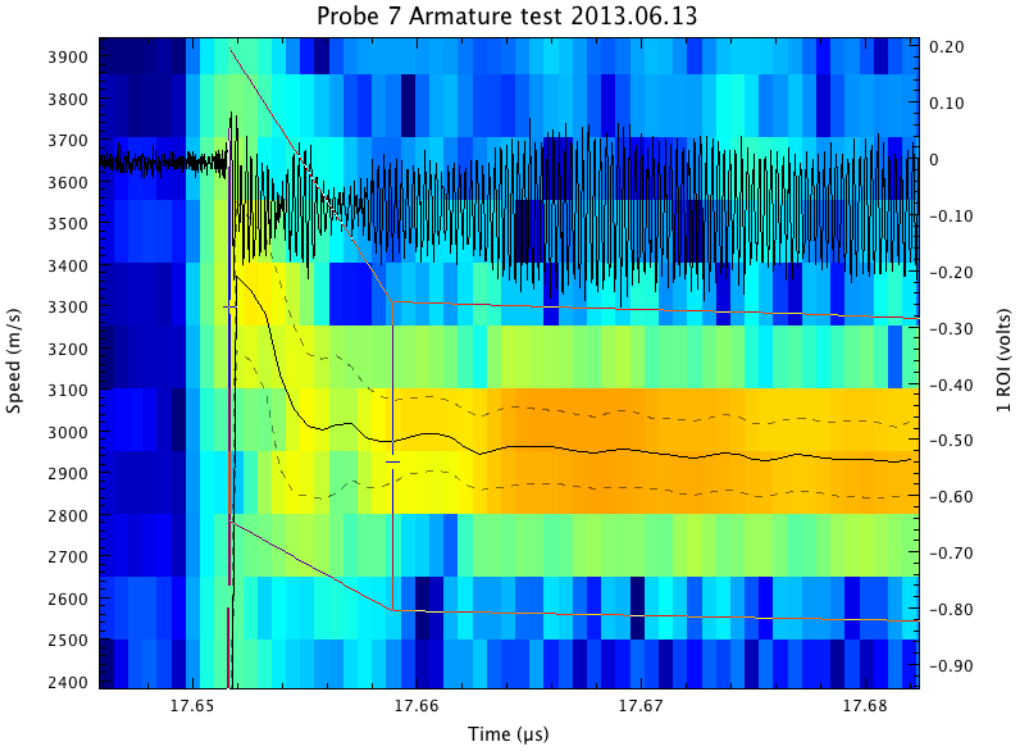

All the probes in the 1—7 radial array showed similar behavior; time is corrected in all the following plots

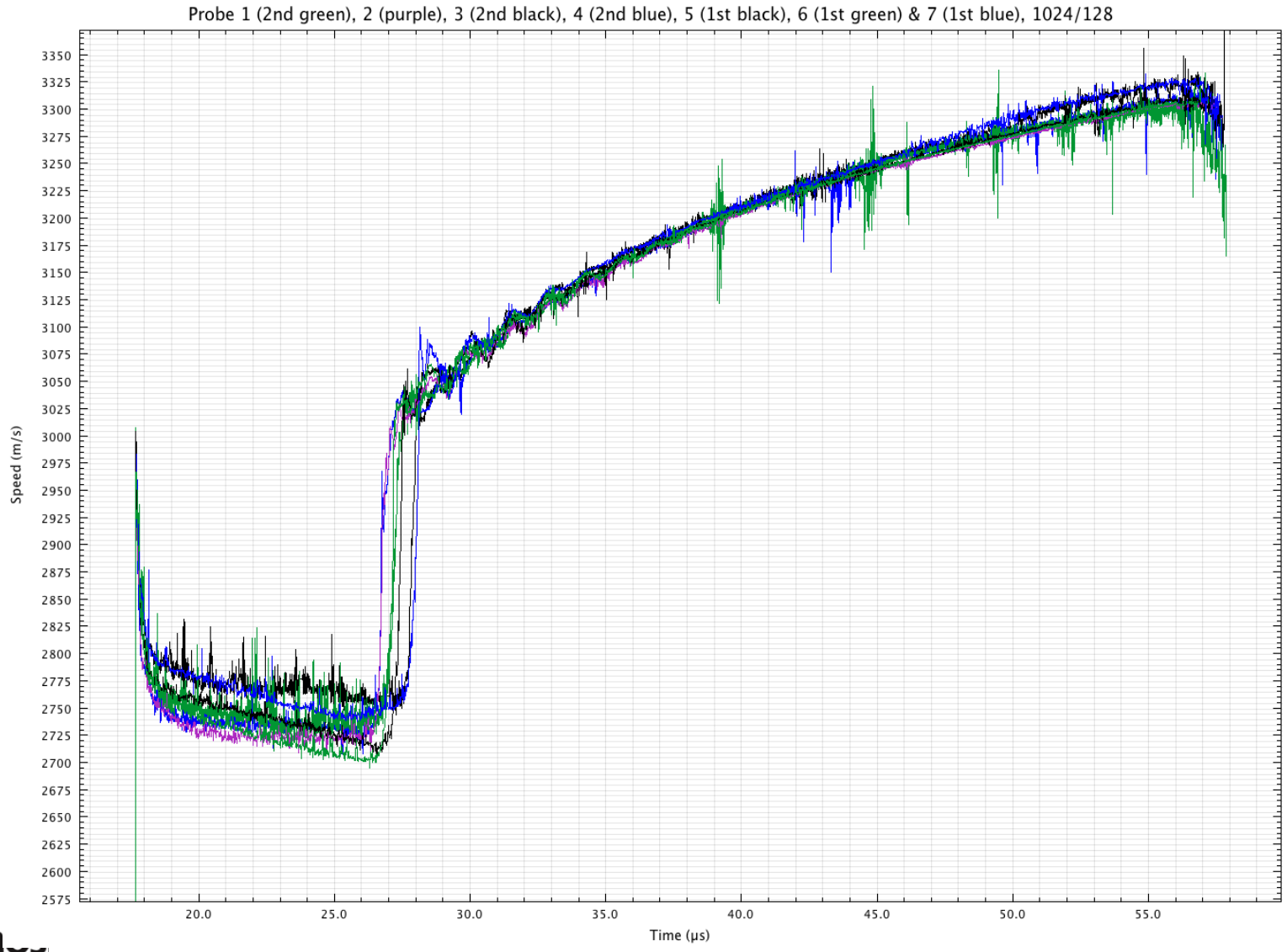

The peak velocity seems to arrive slightly later than the start of motion- difficult to say if real or artifact of analysis; The jump off times are partially scrambled in the analysis by the ± 5 ns spectrogram bins; for jump off, refer to the results taken directly from the oscilloscope traces shown in a scatter plot earlier.

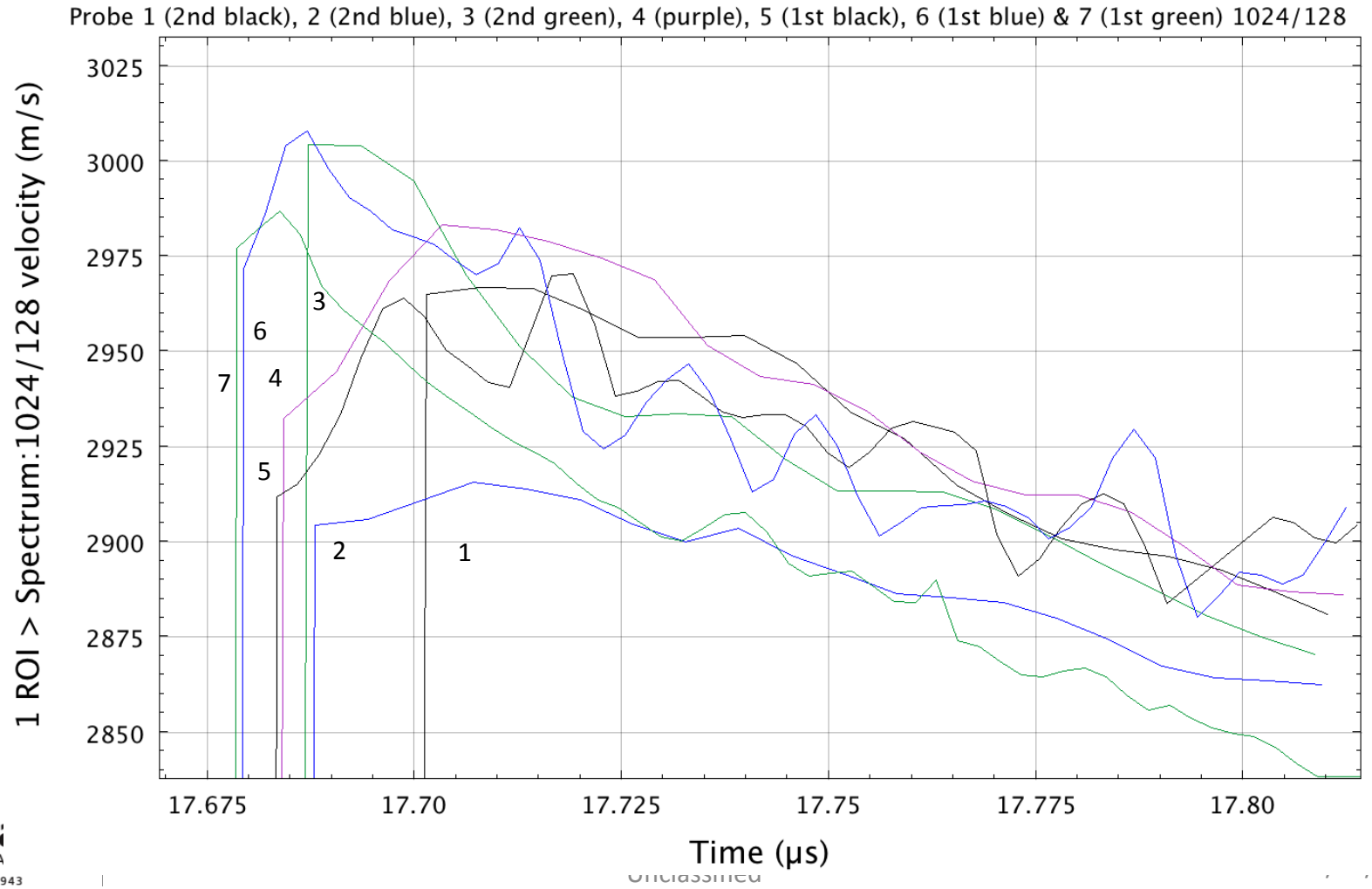

The radial probes 90° off the array of 7 start within 20 ns of each other, but about 350 ns later than the 7 and about 200 m/s faster. The re-shock arrives 2 µs later at the pair 90° below the 7 compared to the pair above.

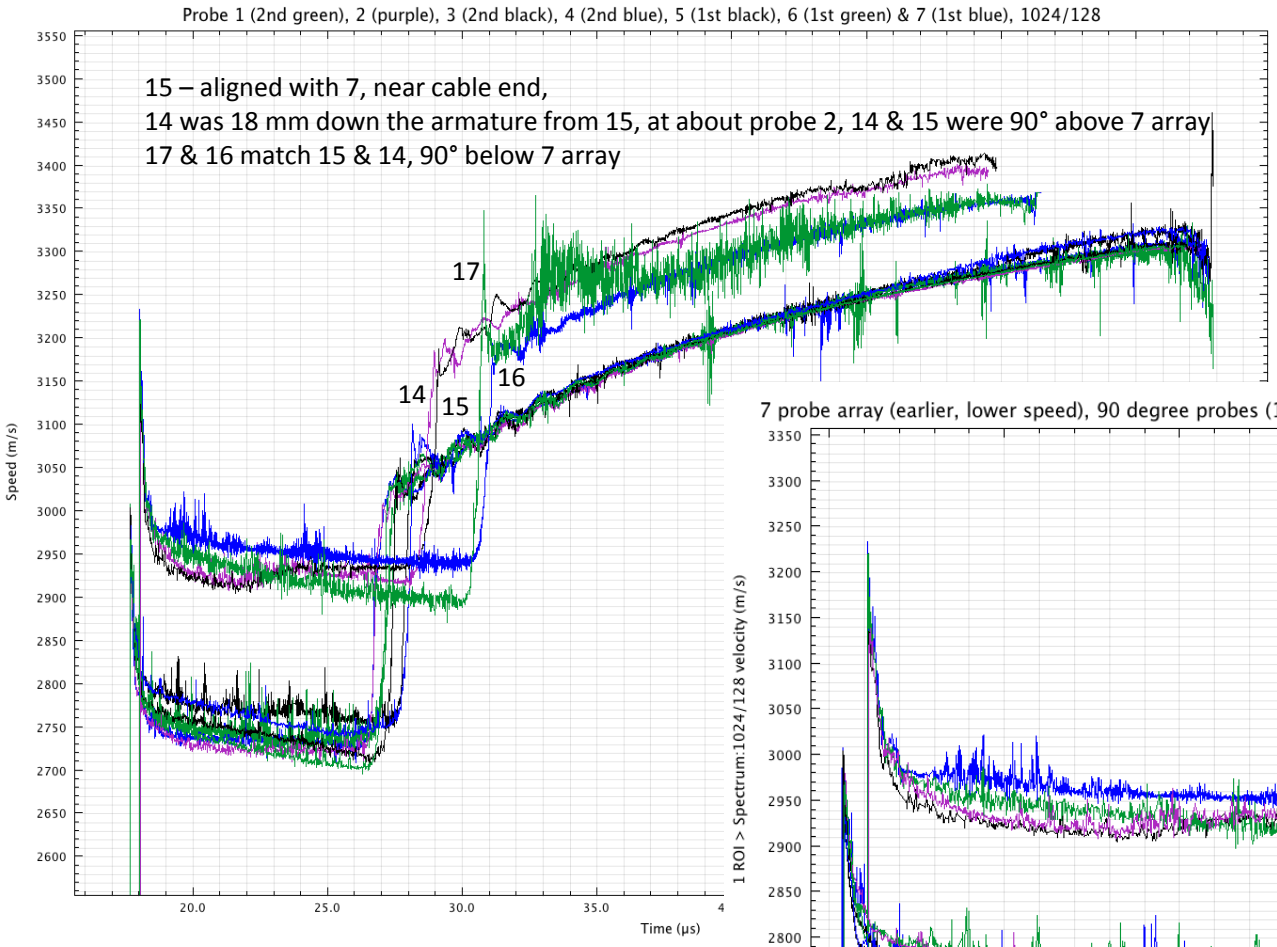

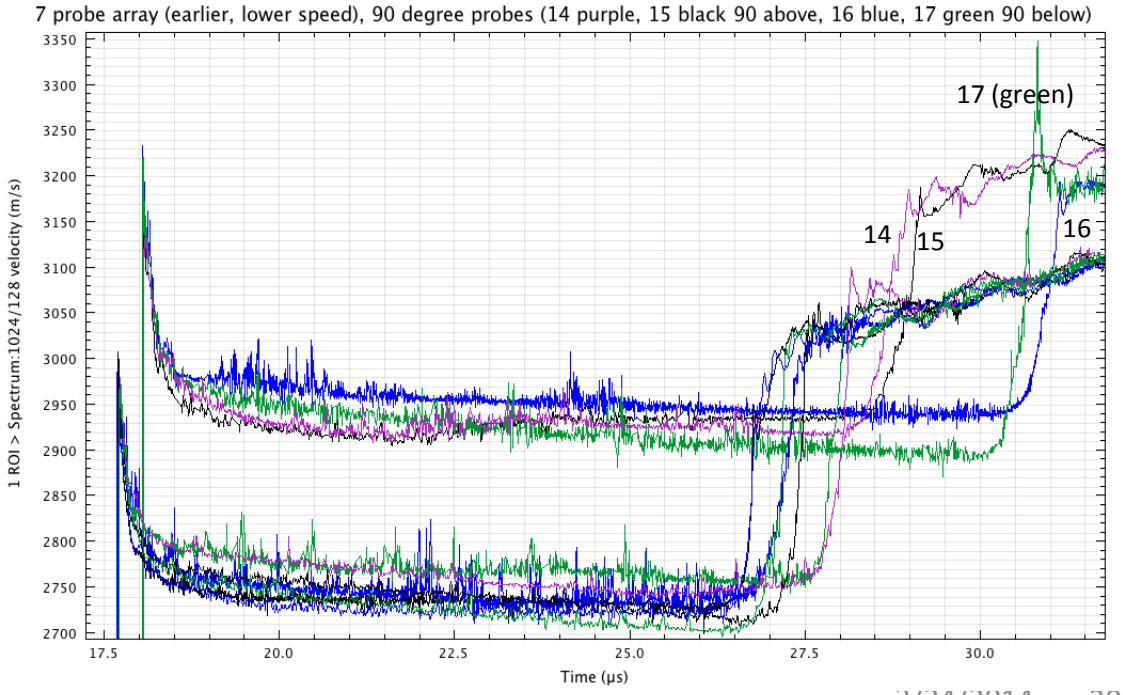

Zoom of the 7 probe array in the re-shock region; note that these shifts are significantly larger than the uncertainty in timing that arises from the width of the spectrogram bins.

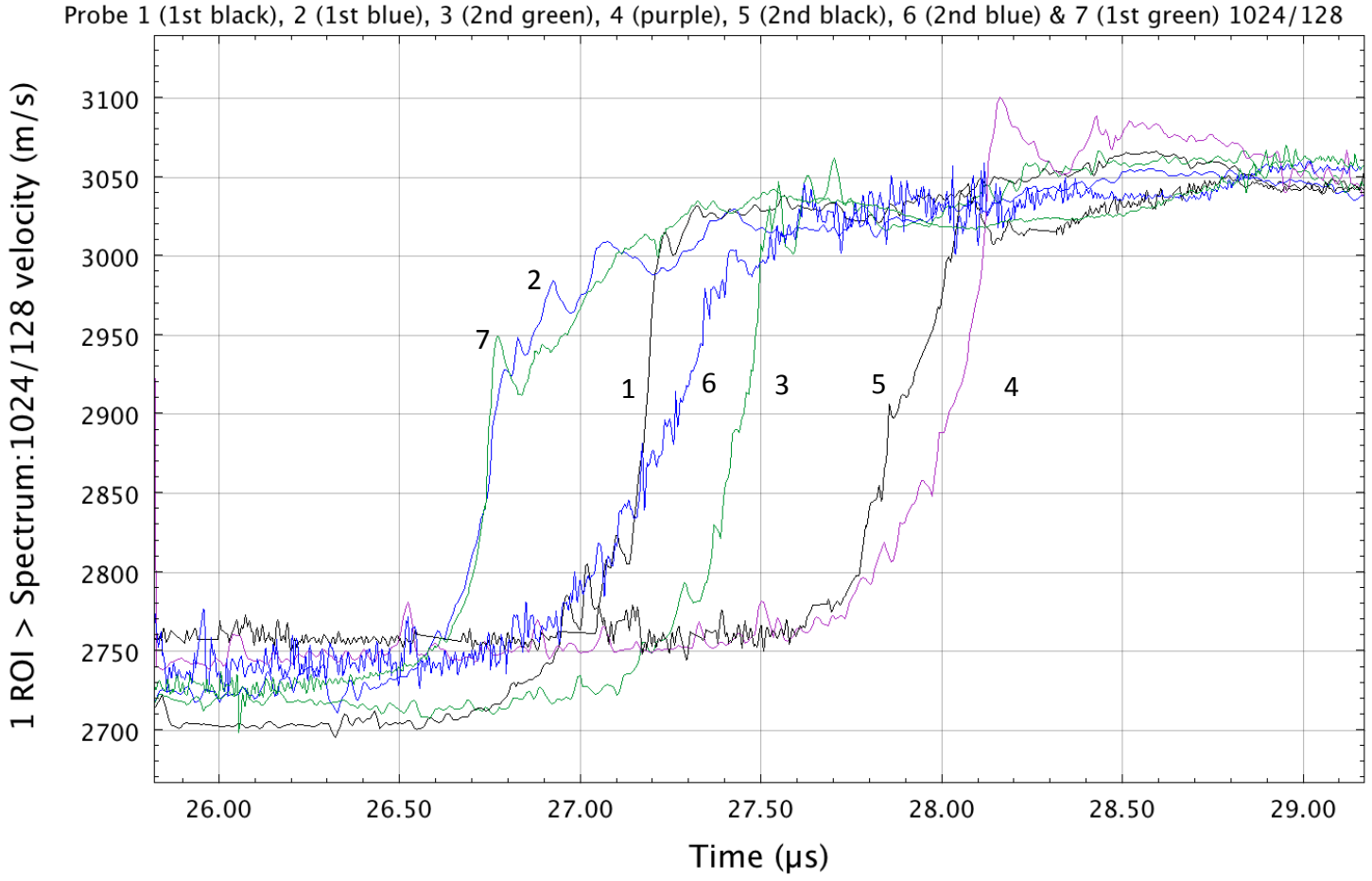

Speed at displacement of 75 mm = 3250 m/s

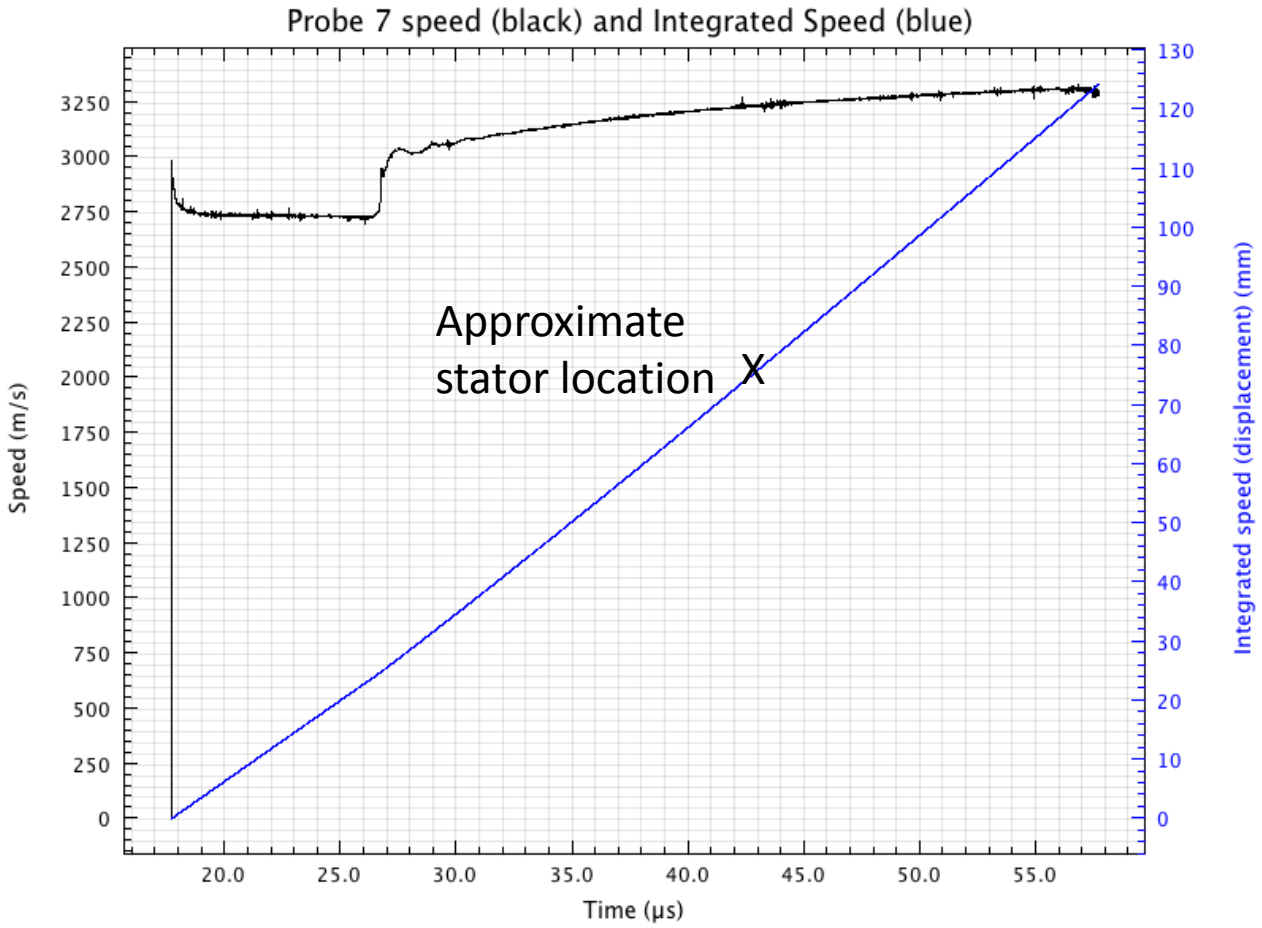

Measured angles were very close to design

The array of 7 radial probes were evenly spaced over 20.8 mm, 3.5 mm ± .2 mm between probes, starting at 218 mm, ending at 238.85 mm. The two probe arrays had probes at 218 and 236 ± .2 mm. The measurements for the angled probes are shown below.

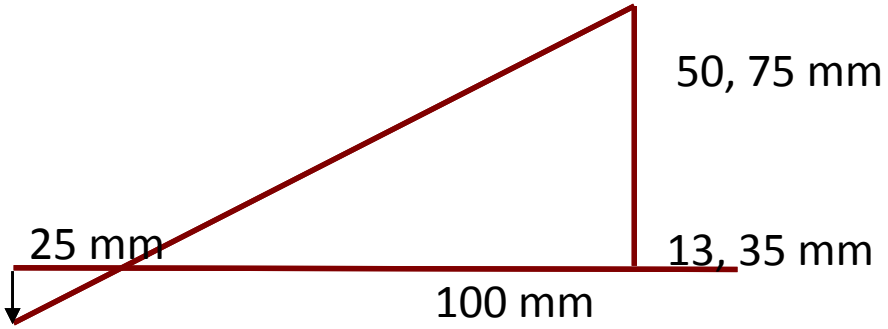

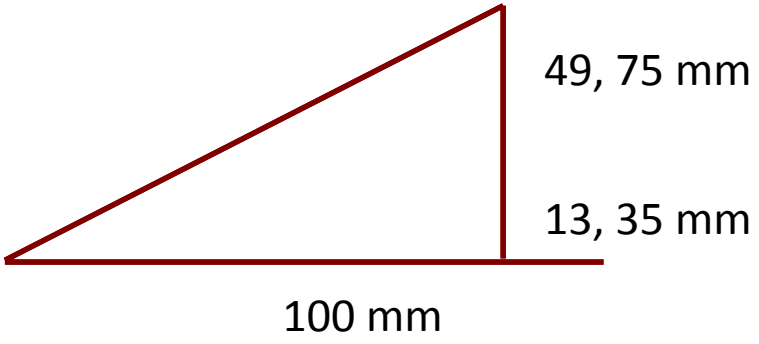

Horizontal angled beams:
θ = tan-1(50/87) = 29.9°
θ = tan-1(75/65) = 49.0°
Sweep = 25tan(29.9)= 14.4
And 28.8 mm.

Vertical angled beams
θ = tan-1(49/87) = 29.4°
θ = tan-1(75/65) = 49.0°

Uncertainties in orientation of one probe relative to another and of the array as a whole

Probe and cross point uncertainty ± .25 mm

Array uncertainties ± 1 mm

Individual probe uncertainty is ± 0.5/100 = ± .005 rad = ± 0.3°

Entire array could be tilted ±2/125 = ± .016 rad = ± 1°, and be displaced in any direction by 1 mm. (Note that the 50° ray missed the cylinder by < ~ 1mm. The rays coming in along the axial direction had the same uncertainties.)

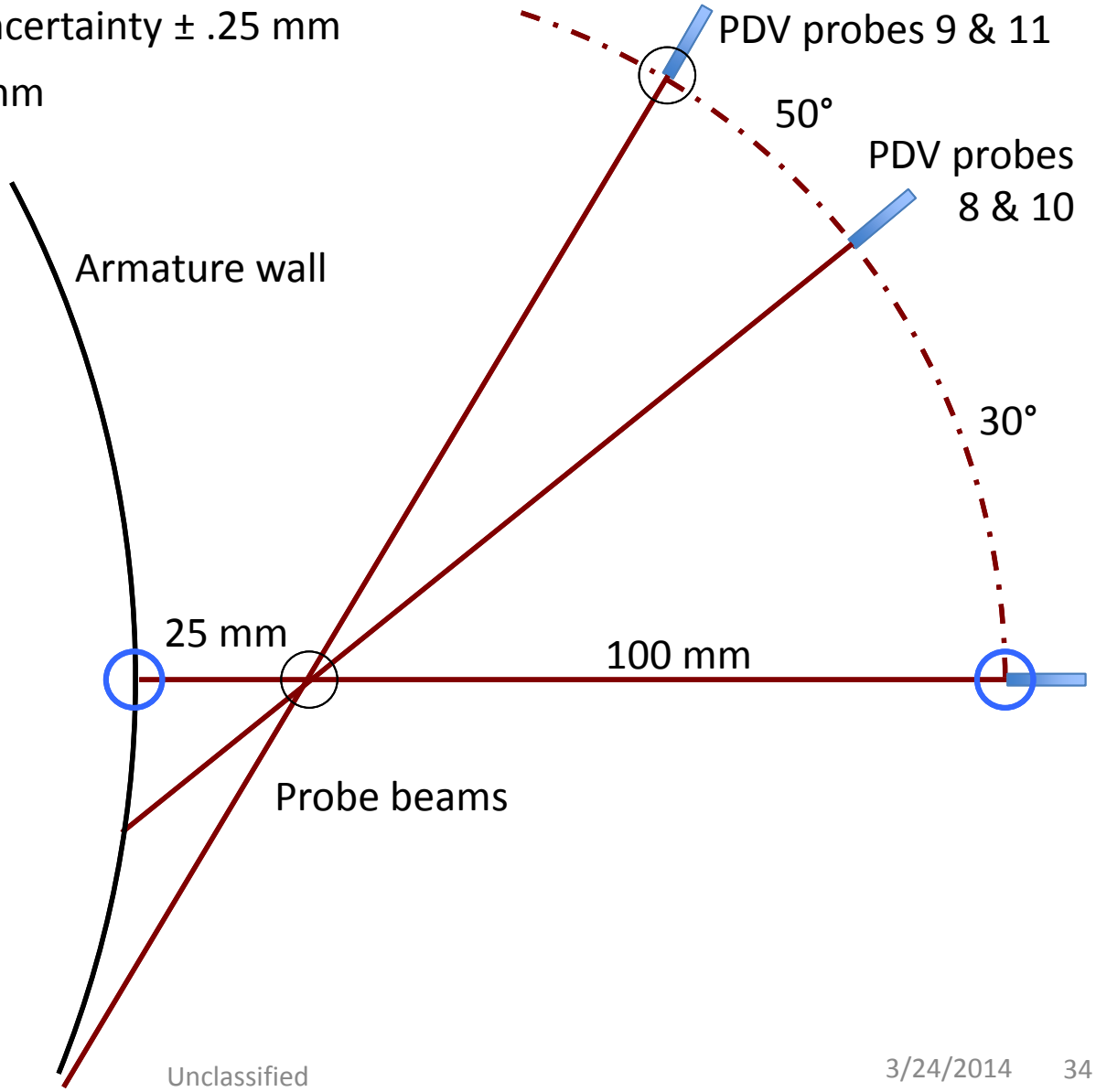

PDV data conclusions

- 7 prove array jump off times were all within 7 ns. Expected “point-to-point” ripple not seen. Possibly because of detonator point-to-point jitter.
- Velocity at armature impact position is 3.25 mm/μs.
- Probes parallel to cables (perpendicular to slapper direction) showed motion ~350 ns later than those looking perpendicular to cable. On this test we looked from both sides to rule out slapper alignment issues. Apparently cables were centered, and there is a lag due to some aspect of propagation perpendicular to slapper shock direction. This was seen looking from one side only on LA-43-CT-1, and is not a feature due to eliminating the smoothing layer. Apparently Ranchero performance is not significantly effected by the 350 ns delay.
- Armature will contact stator ~25 μs after first motion.
- Data seem to confirm that armature spalls.
  - That is, there is an abrupt jump off, followed by a relatively low (2.75 mm/μs) coasting phase
  - Recollection occurs after about 10 μs, and recollects first over det points and last over interaction points
- The difference between Kapton signals on LA-43-2 and LA-43–CT-2 are not understood at this time.
- The ability to field multiple channels of PDV on tests like these provides a major increase in the level of precision and understanding that result from a test. This information can be folded into modern computational capability to yield an increased fidelity of computational results.

Camera Records

- X-ray inspection data to locate bubbles
- Cooke Framing Camera Data
- Phantom Data

Bubble “one” azimuthal location

- Visible features on radiographs are measured with a ruler on a light table and plotted manually.
- Bubble distances from an identifiable feature (e. g. the armature) are obtained for three different angles.
  - Perpendicular to cable
  - Parallel to cable
  - 45˚
  - Error in angle on 45˚ view is substantial
- Right and left are discerned from asymmetric cable clamp.
- Three positions intersect at bubble location. Error in angle gives rise to uncertainty in position.

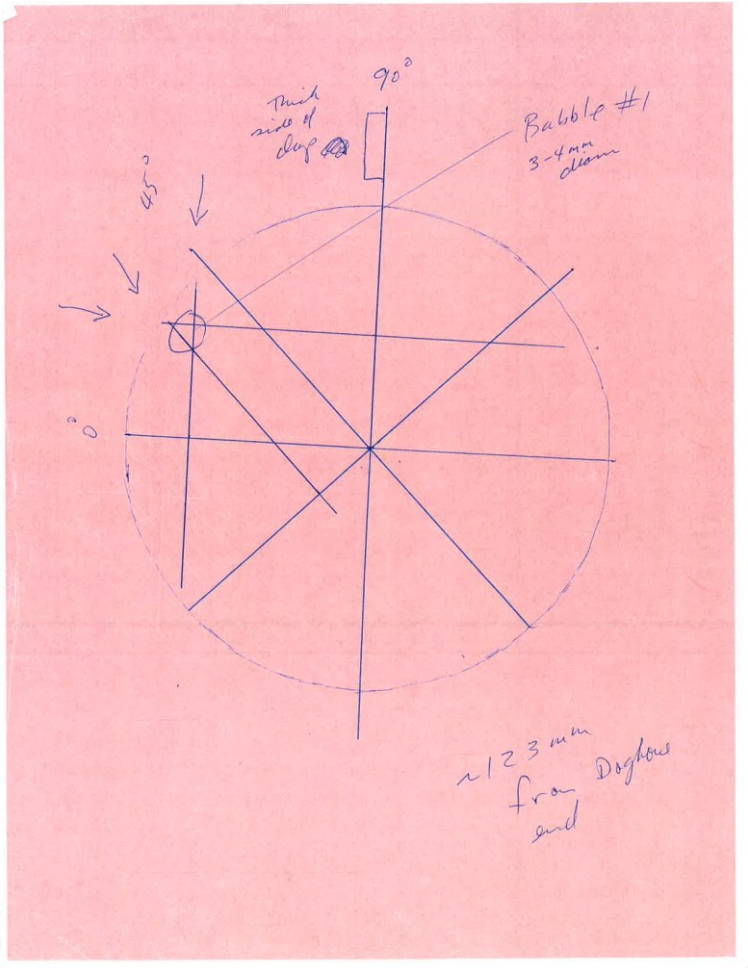

Bubble “two” azimuthal location

- Visible features on radiographs are measured with a ruler on a light table and plotted manually.
- Bubble distances from an identifiable feature (e. g. the armature) are obtained for three different angles.
  - Perpendicular to cable
  - Parallel to cable
  - 45˚
  - Error in angle on 45˚ view is substantial
- Right and left are discerned from asymmetric cable clamp.
- Three positions intersect at bubble location. Error in angle gives rise to uncertainty in position.

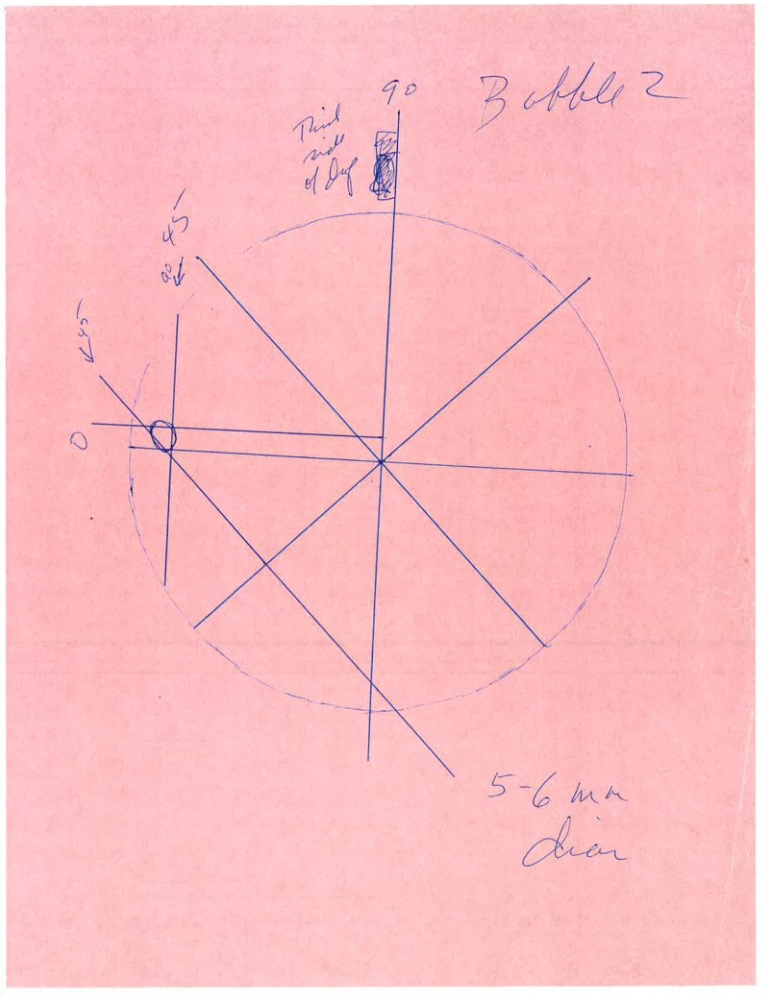

Bubble “three” azimuthal location

- Visible features on radiographs are measured with a ruler on a light table and plotted manually.
- Bubble distances from an identifiable feature (e. g. the armature) are obtained for three different angles.
  - Perpendicular to cable
  - Parallel to cable
  - 45˚
  - Error in angle on 45˚ view is substantial
- Right and left are discerned from asymmetric cable clamp.
- Three positions intersect at bubble location. Error in angle gives rise to uncertainty in position.

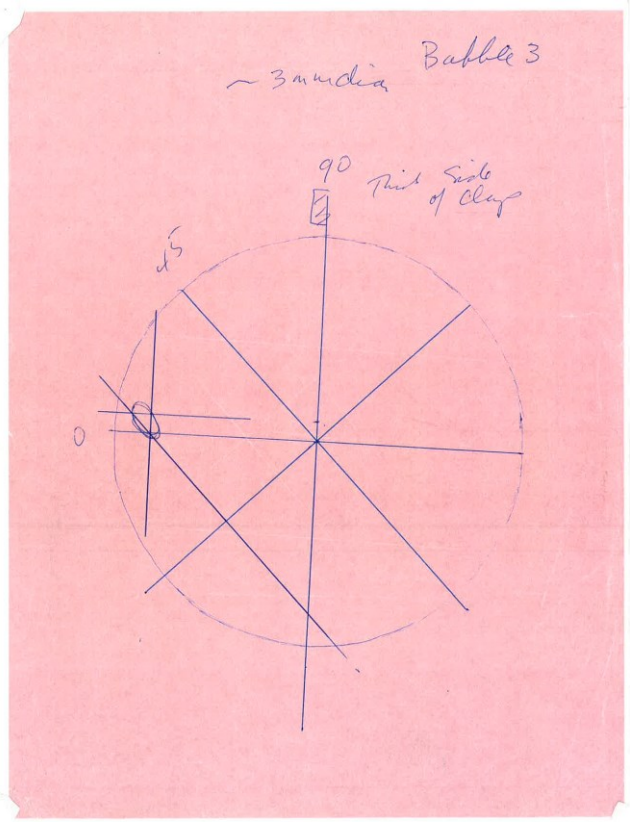

Z- location of bubbles

- Measurements made using ruler and light table
- Z- position of bubbles could be measured from one end of HE in armature.
- Parallax gives rise to error
- Note on the original hand drawing shown here recognizes that one slapper solder joint shows up more than the rest – no poor performance resulted

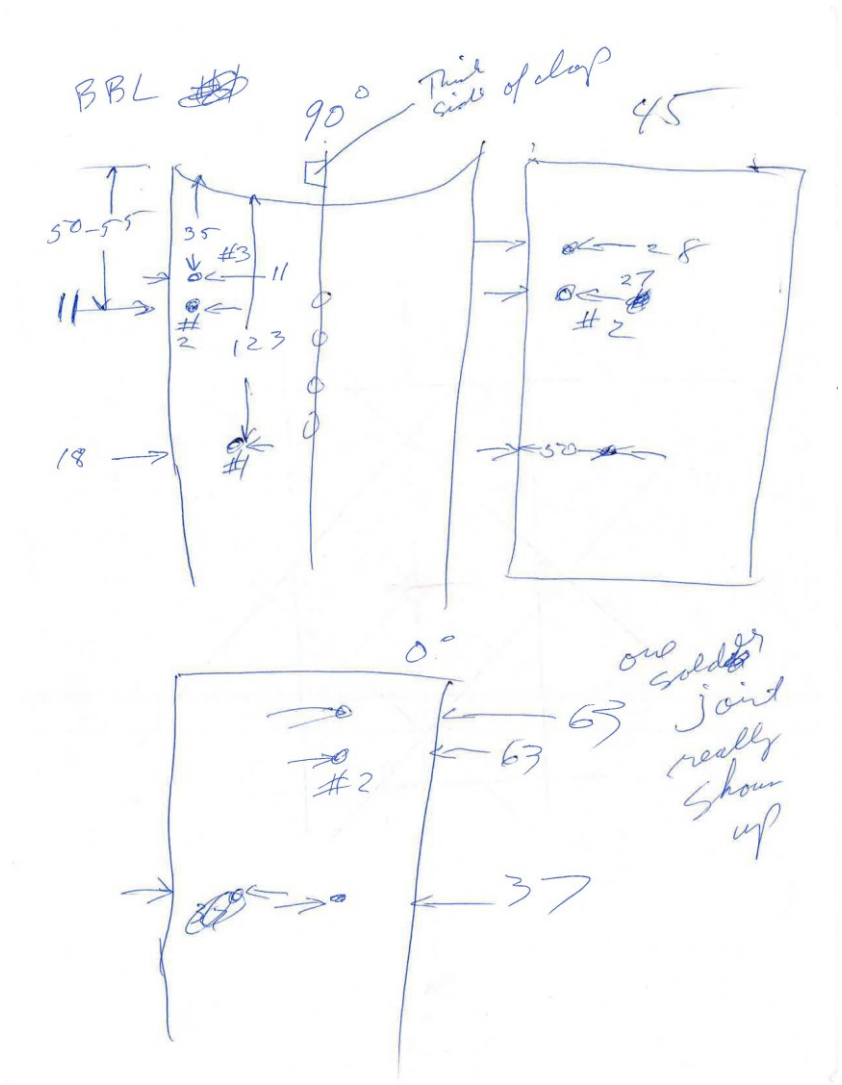

Bubble positions were projected before the shot based on the x-rays described above

- With bubble azimuth and z-position located, projections were made for locations that would rupture on the shot.
- The cable was to be oriented as shown, facing down at a 45˚ angle
- Note that decision to move further away from bubbles with PDV sensors was rejected. This was considered in case the right/left determination made off the x-rays was not correct. In the end confidence in getting this correct improved and the original location was used.

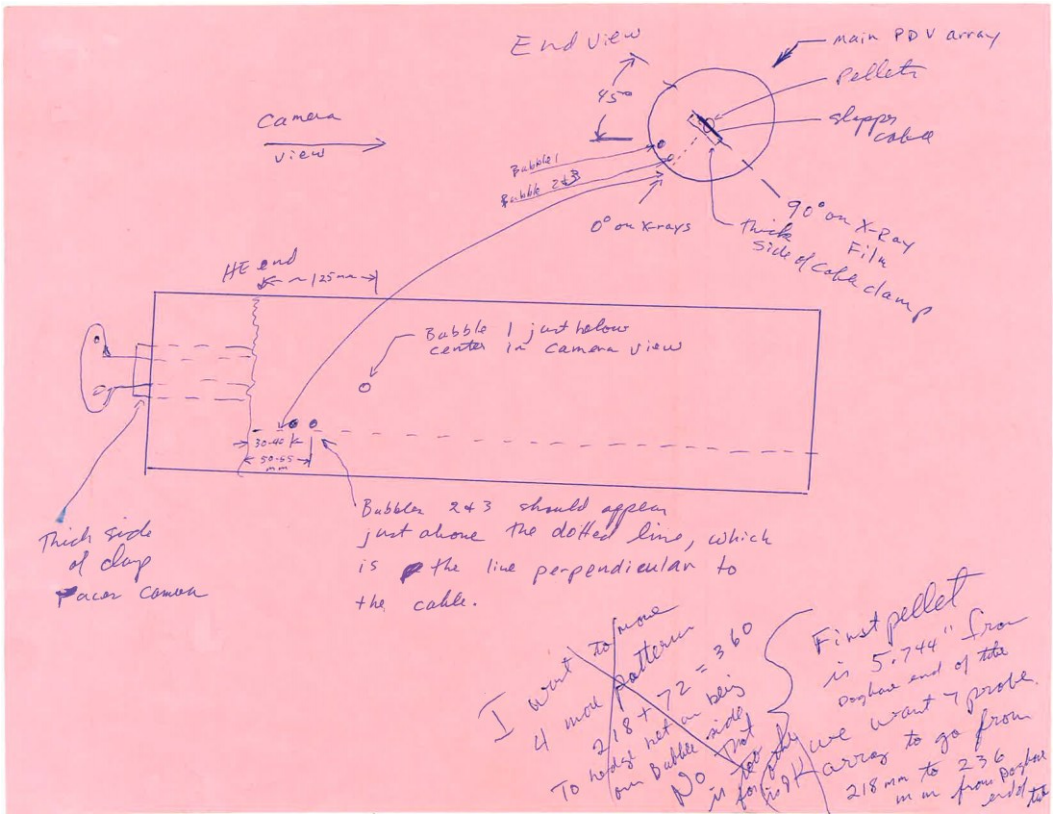

Cooke Camera Data and absolute timing

- Mark Marr-Lyon

Time relative to CVR - shock switch closed late.

In earlier work (LA-43-2 – 9/11) it was discovered that our shock switches were exhibiting a bi-modal closing times. A newer lot of switches was used for LA-43-2, but that lot also showed the bi-modal performance until the firing unit voltage was increased to 8 kV. No late closures were seen with that lot at the higher voltage. The older lot was used here, because absolute timing was unimportant and the remainder of the new lot needed to be used for a DAHRT test. The late closure was observed here, and this is the first occurrence of this since it was decided to raise the firing unit voltage to 8kV for LA-42-2.

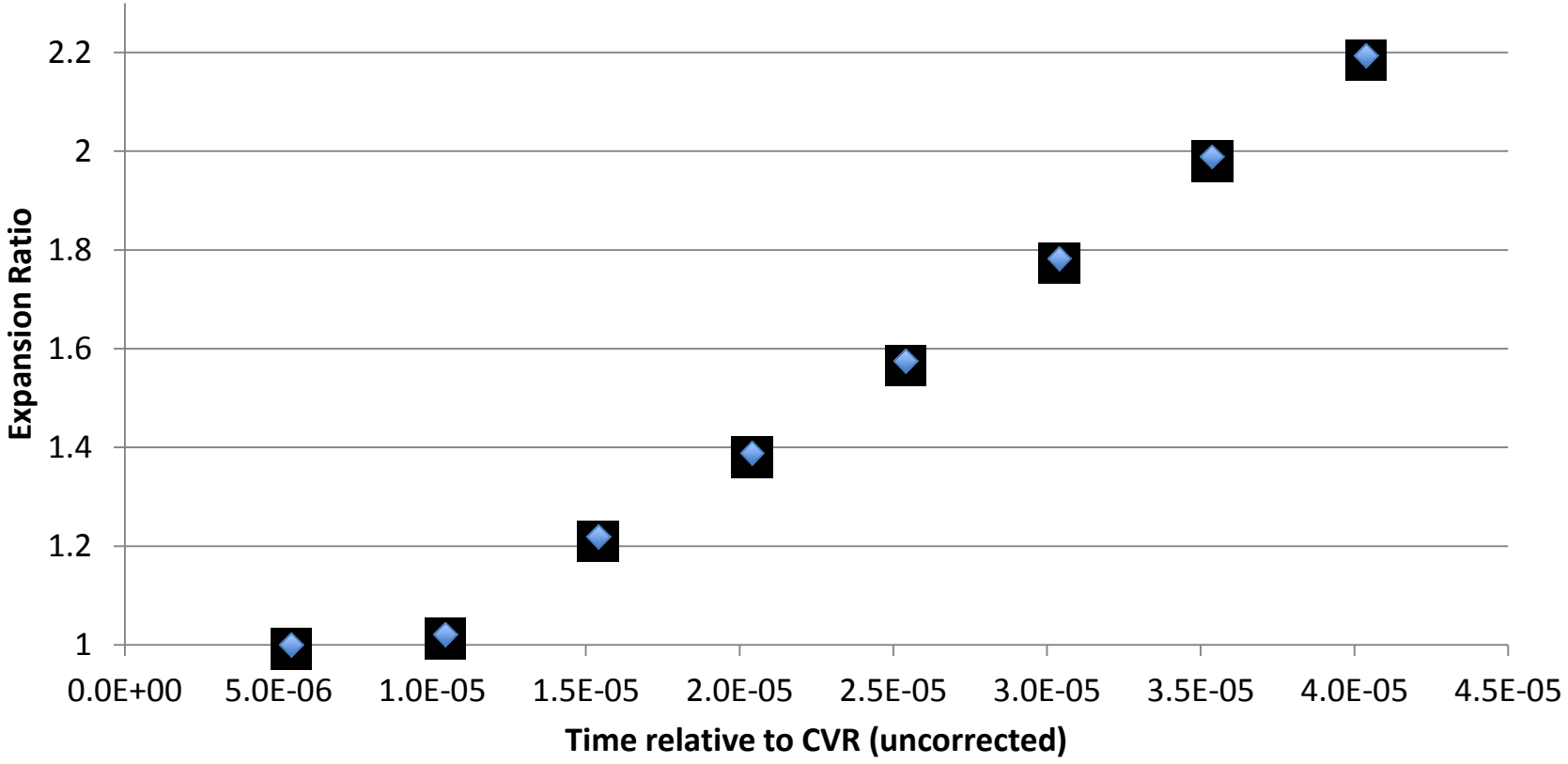

Cooke Parameters

- Cooke camera has independently triggerable frames, but we chose to trigger frames at fixed intervals starting with a frame ~5 μs before armature first motion. The result of the late shock switch closure is that frame 2 occurs when armature has moved only a small amount.
- Array size is 1280x1024.

Cooke frame 1; before 1st motion

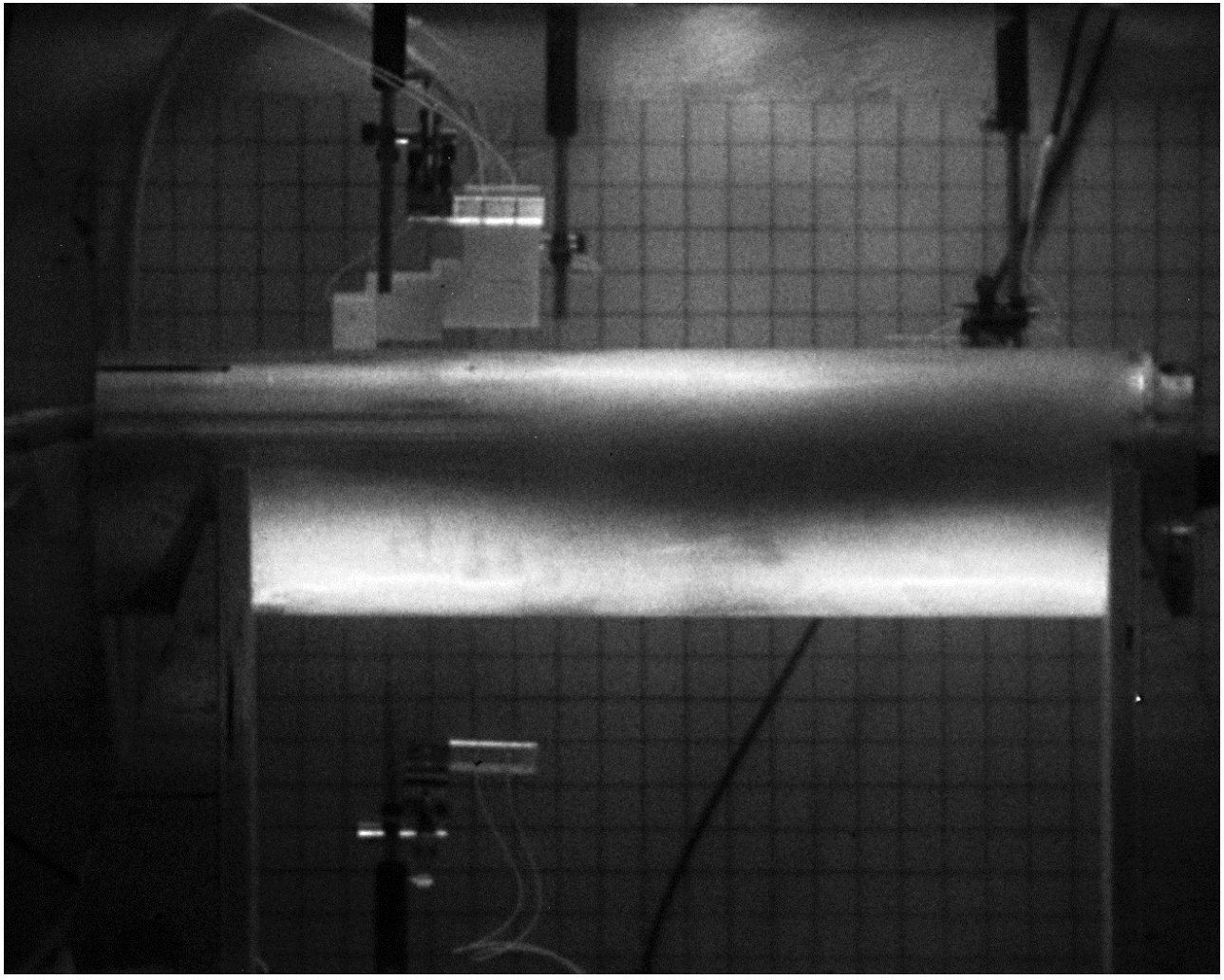

Cooke frame 2; ~ 0.3 µs after 1st motion

The left hand side of this image is the uncontrolled end of the casting, which is always located at the input end of a Ranchero. The input glide plane eliminates any issue due to these asymmetries in a Ranchero device. It is also worth noting that there is a slight non-uniformity at the other end in the same location, which is roughly at the 90 degree location (probes 14-17) shown in the PDV data.

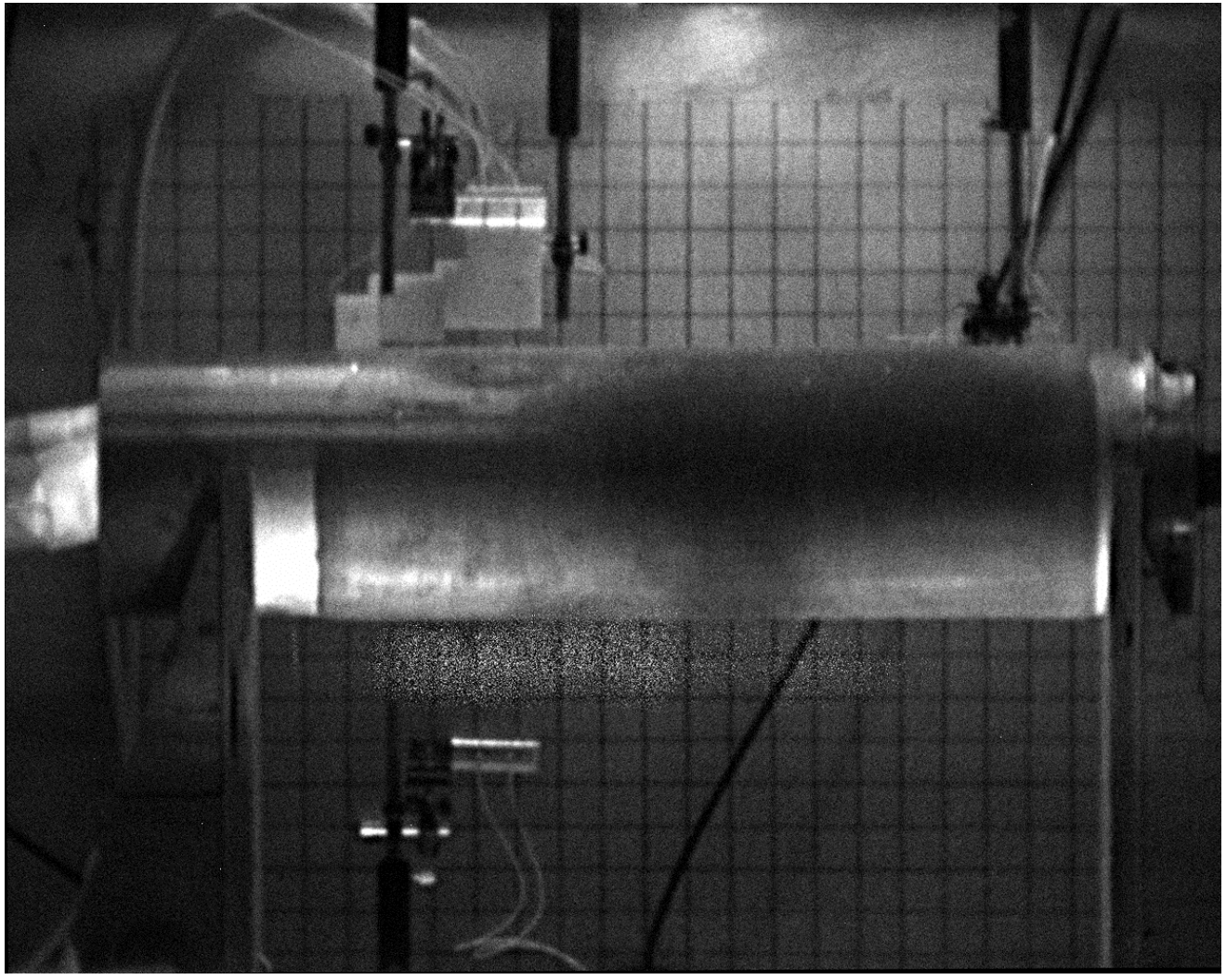

Cooke frame 3; ~ 5.3 µs after 1st motion

First visual indication that known bubbles would show up

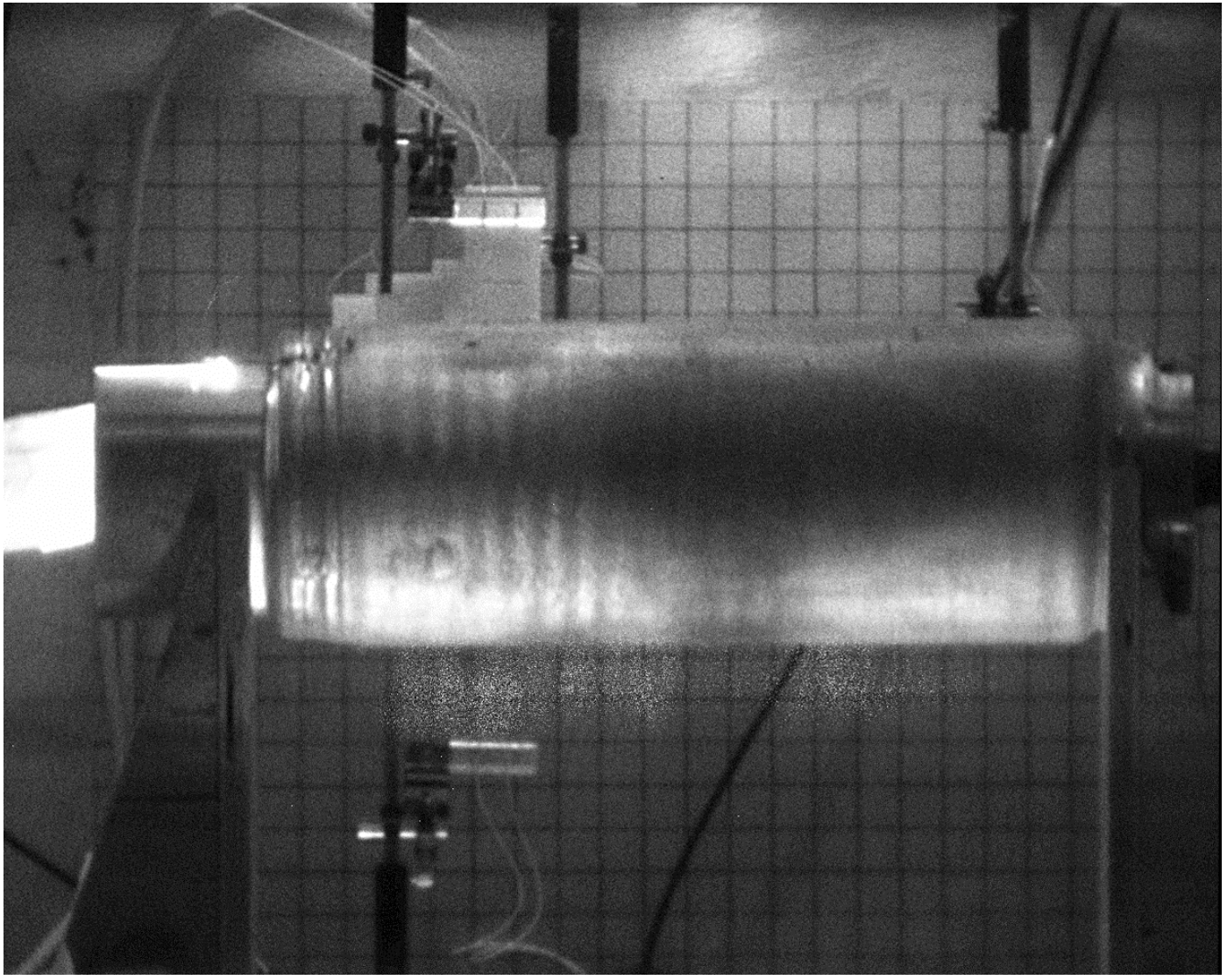

Cooke frame 4 ; ~ 10.3 µs after 1st motion

Bubble 1 shows up as a bright spot. 2 and 3 are not pronounced.

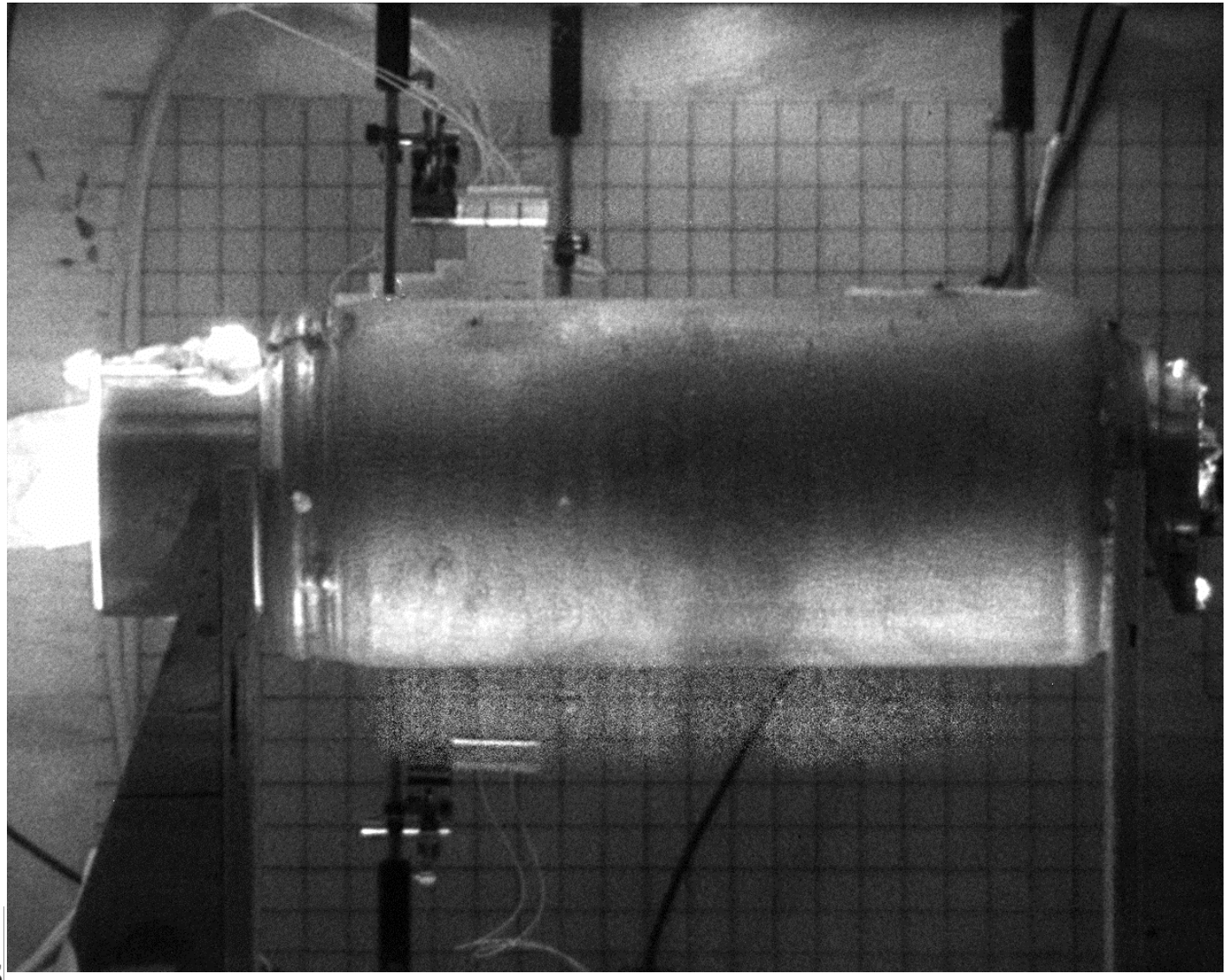

Cooke frame 5 ; ~ 15.3 µs after 1st motion

First evidence that un-predicted blow outs will occur. Bubble 1 shows up here as a bright spot.

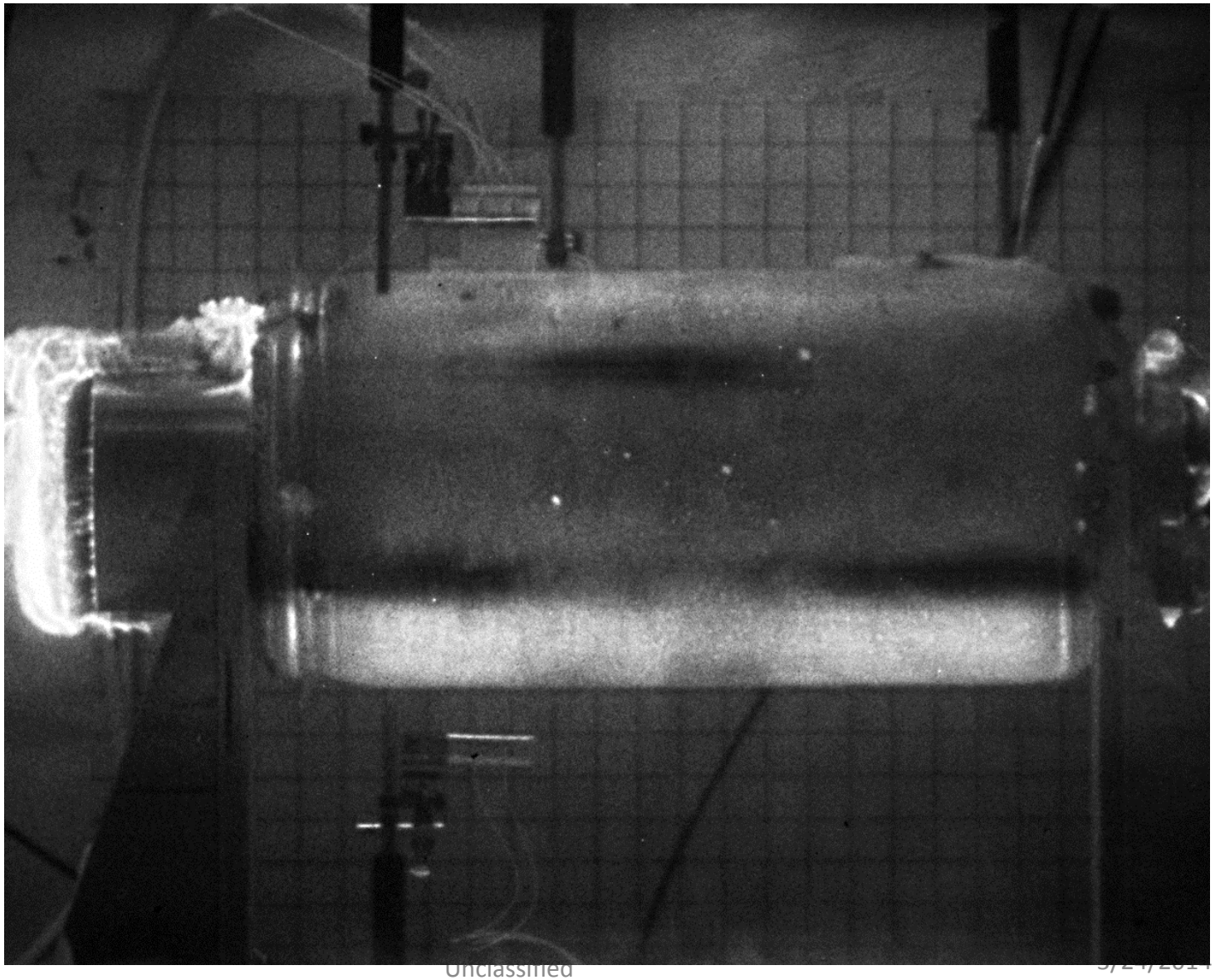

Cooke frame 6 ; ~ 20.3 µs after 1st motion

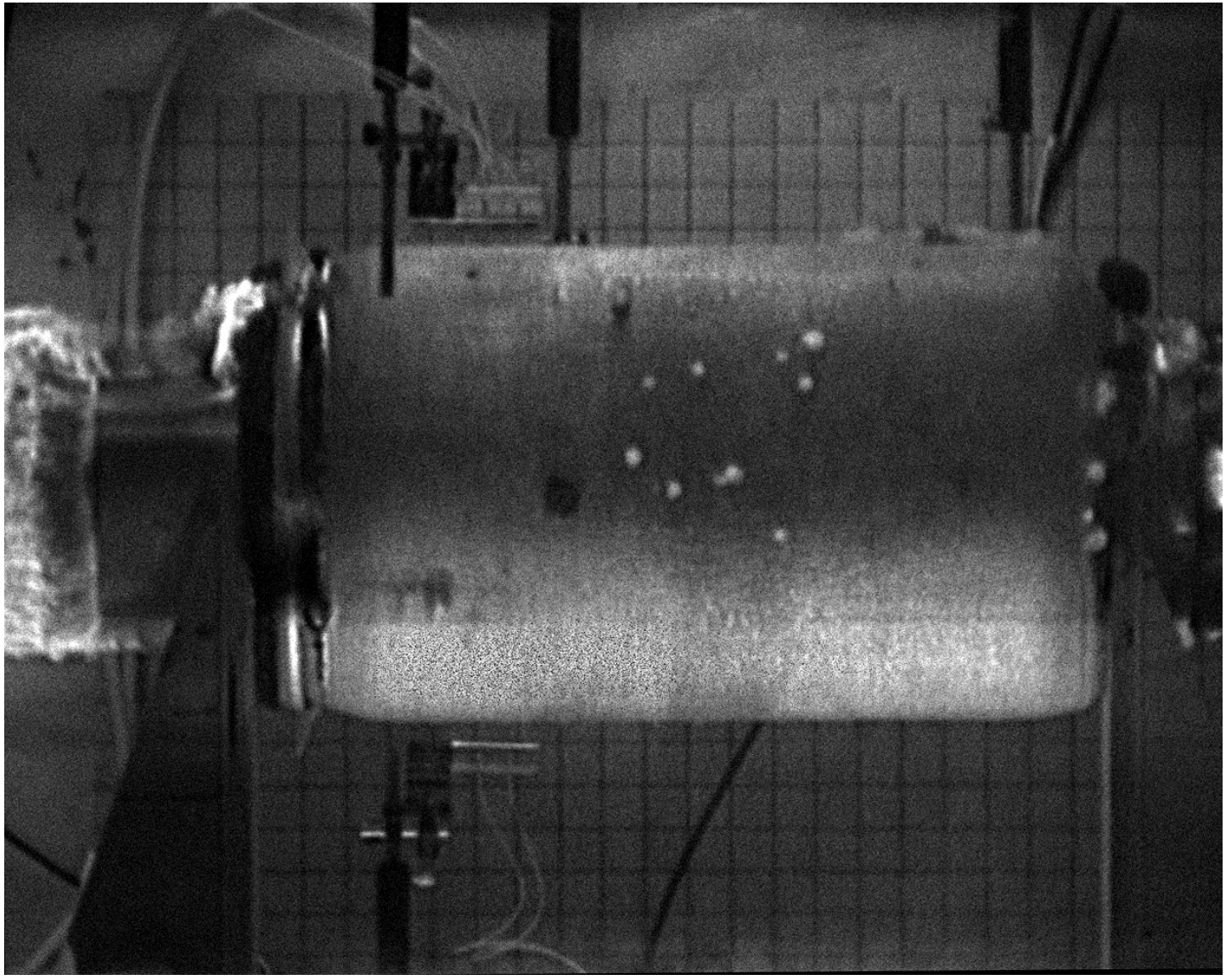

Cooke frame 7 ; ~ 25.3 µs after 1st motion

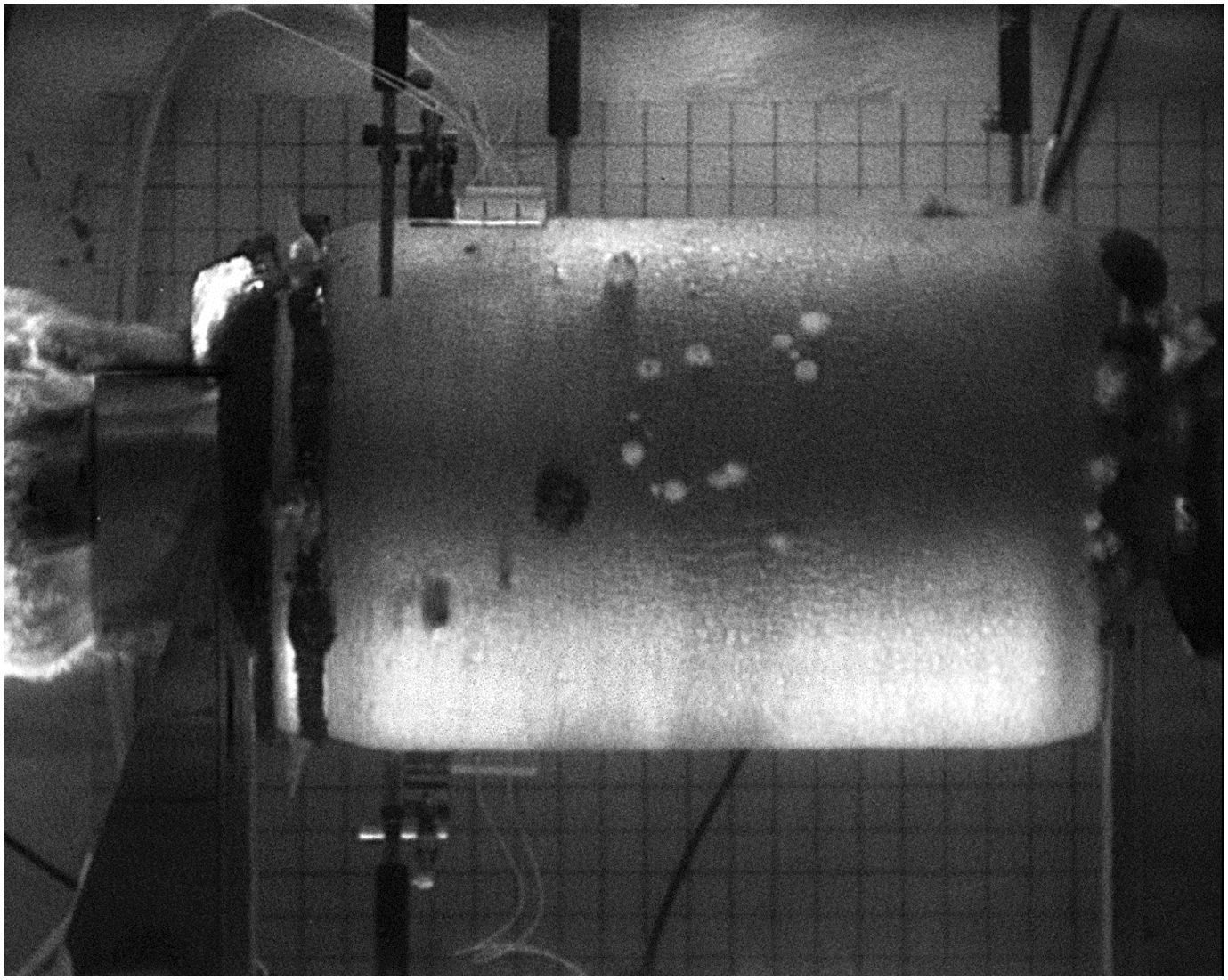

Cooke frame 7 - 2x expansion

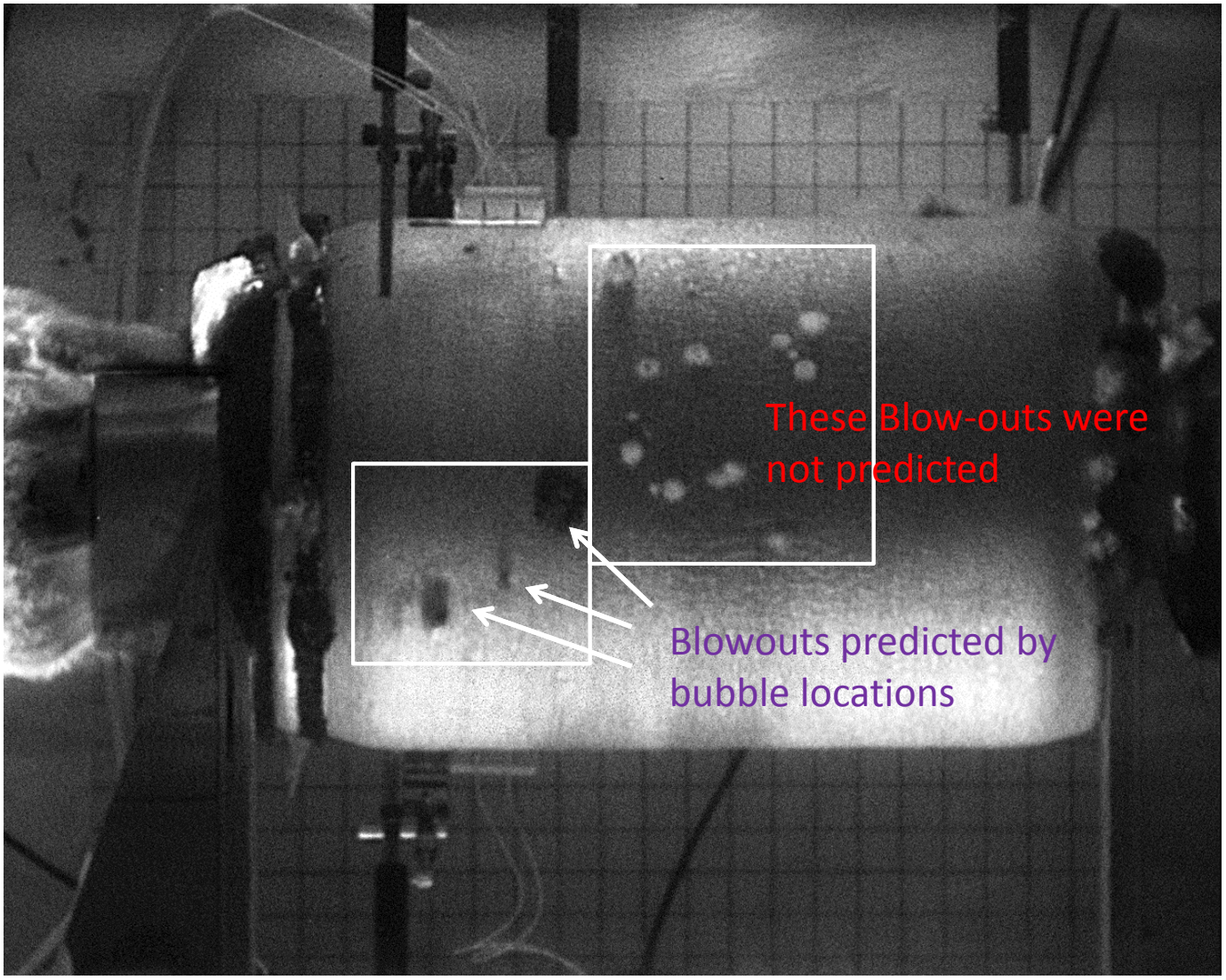

Cooke frame 8 ; ~ 30.3 µs after 1st motion

Visible difference between predicted and unpredicted bubbles persists through this last frame.

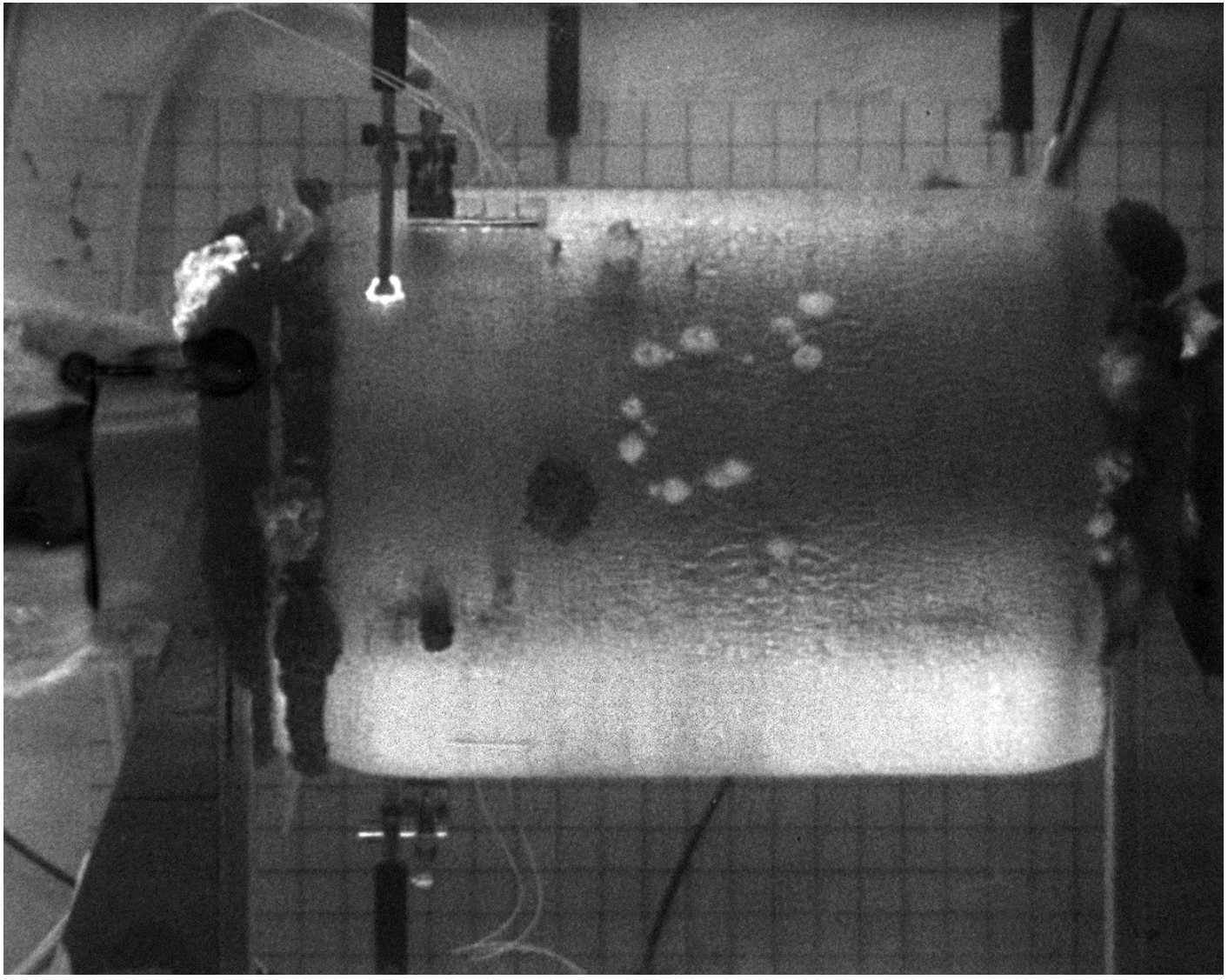

Phantom Data array is 256 x 256

Identifiable features put figure 3 between frames 6 and 7 on the Cooke

PBXN-110 ARMATURE TEST

SHOT 06-13-2013

Summary– High speed camera data (79069 fps, 77.6 mil/px) was collected on a PBXN-110 filled 6 inch diameter, 236.2 mil wall thickness aluminum armature. Imanges were collected at the following diameters normalized to the initial diameter: 1.0, 1.46, and 1.97 as illustrated in Figs 1 – 3 respectively. Failure of the aluminum armature is observed at an expansion factor of 1.46. See white dots in Fig. 2.

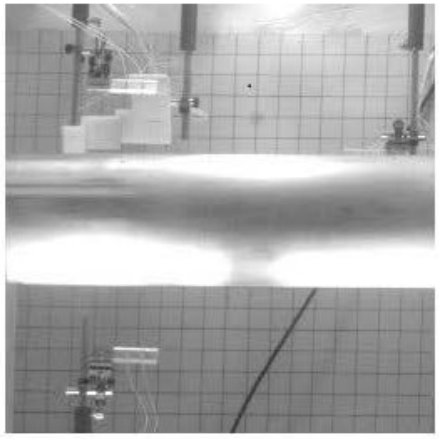

FIG. 1: Image before initiation, t = 0.008 ms with t_{trg}= -0.056 ms. Diameter is 6 inches.

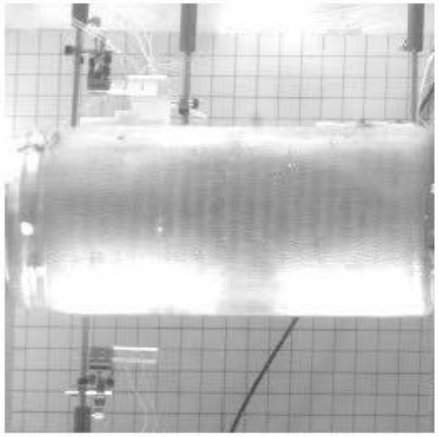

FIG. 2: Image after initiation, t = 0.020 ms with t_{trg}= -0.056 ms. Diameter is 8.75 inches.

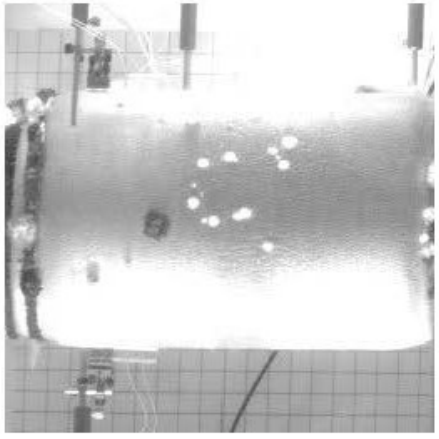

FIG. 3: Image after initiation, t = 0.033 ms with t_{trg}= -0.056 ms. Diameter is 11.85 inches.

Phantom frame 1. Phantom time = 8 µs and it is prior to first motion

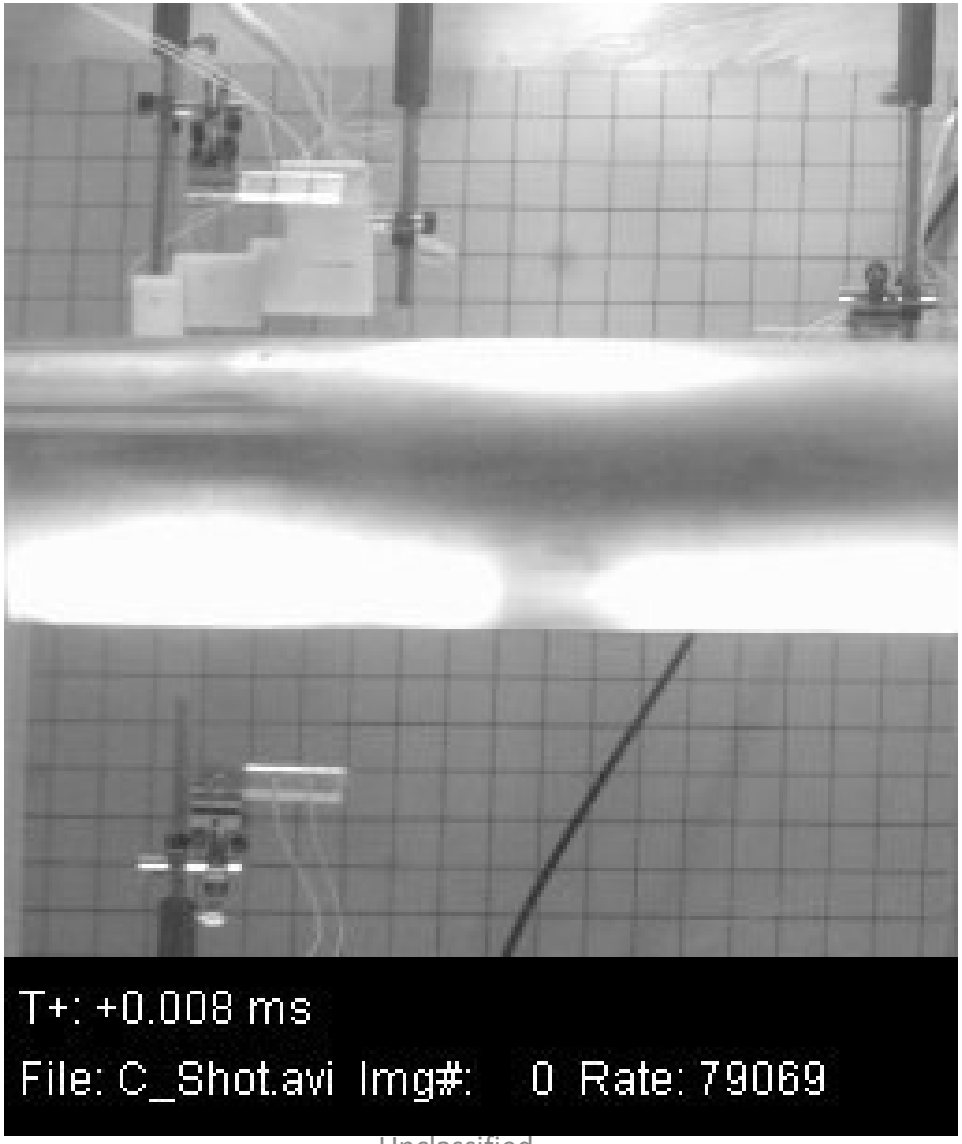

Phantom frame 2 just after frame 4 of the Cooke.
t = 20 µs; Diameter = 8.75”

There are 23 bright ridges on the armature, indicating that they occur in between the pellets rather that over them.

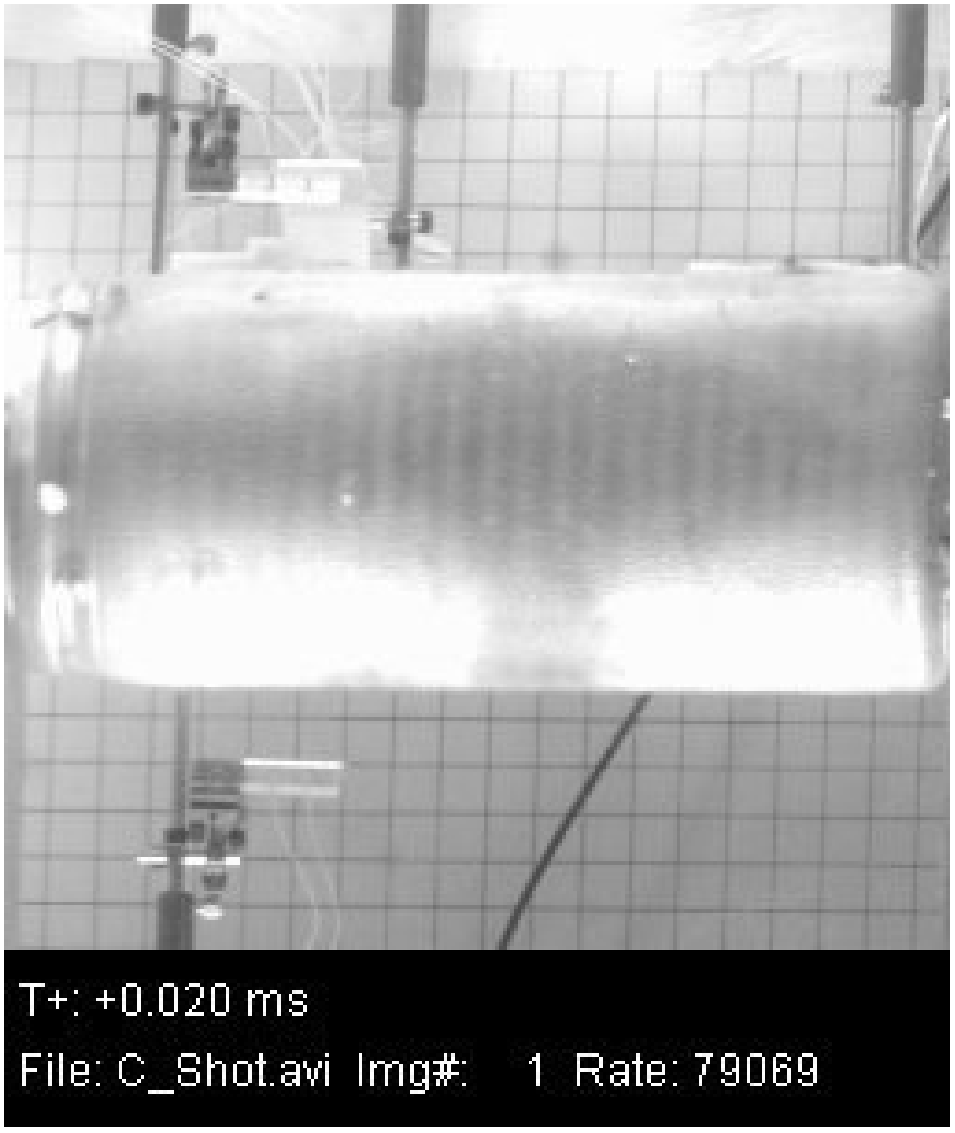

Phantom frame 3 – just before frame 7 of the Cooke. Phantom time = 33 µs. Diameter = 11.85”

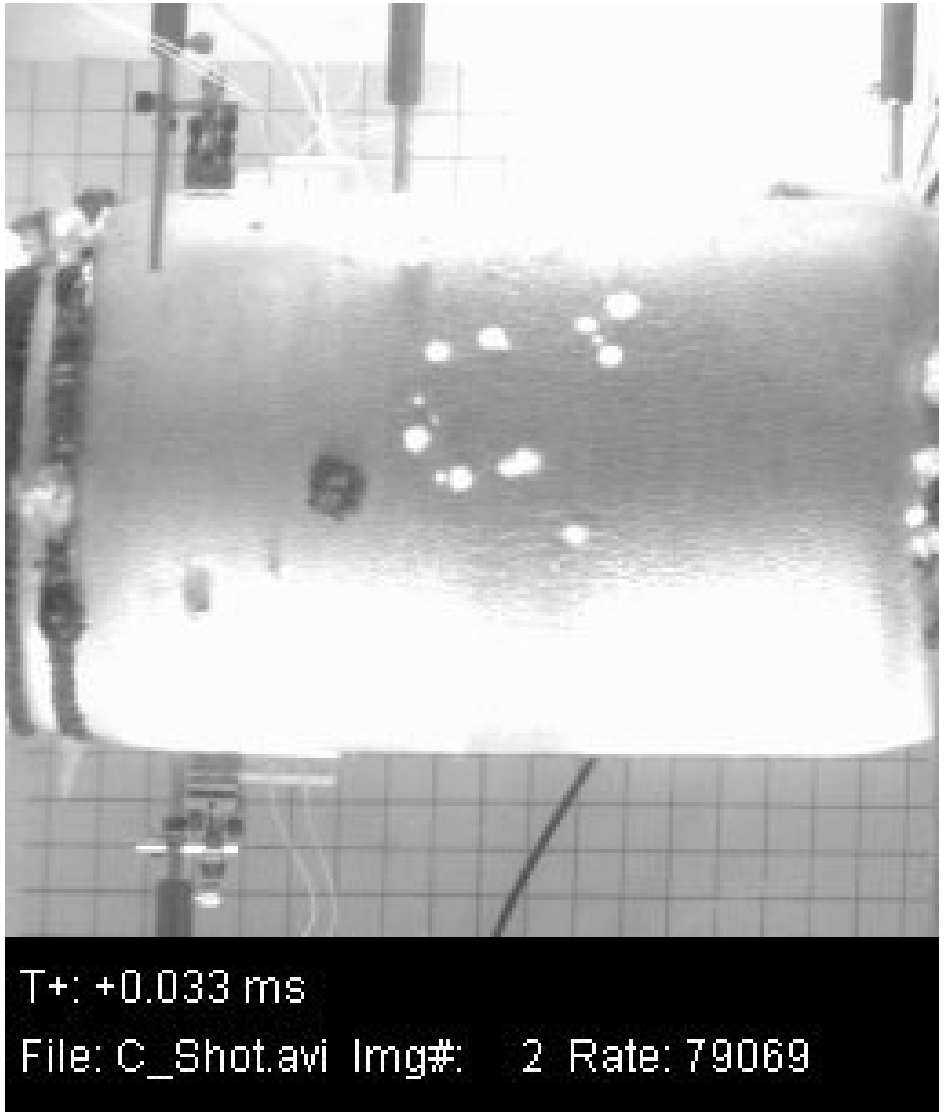

Phantom Frame 4 – After the last Cooke Frame (#8) – Phantom time 46 µs

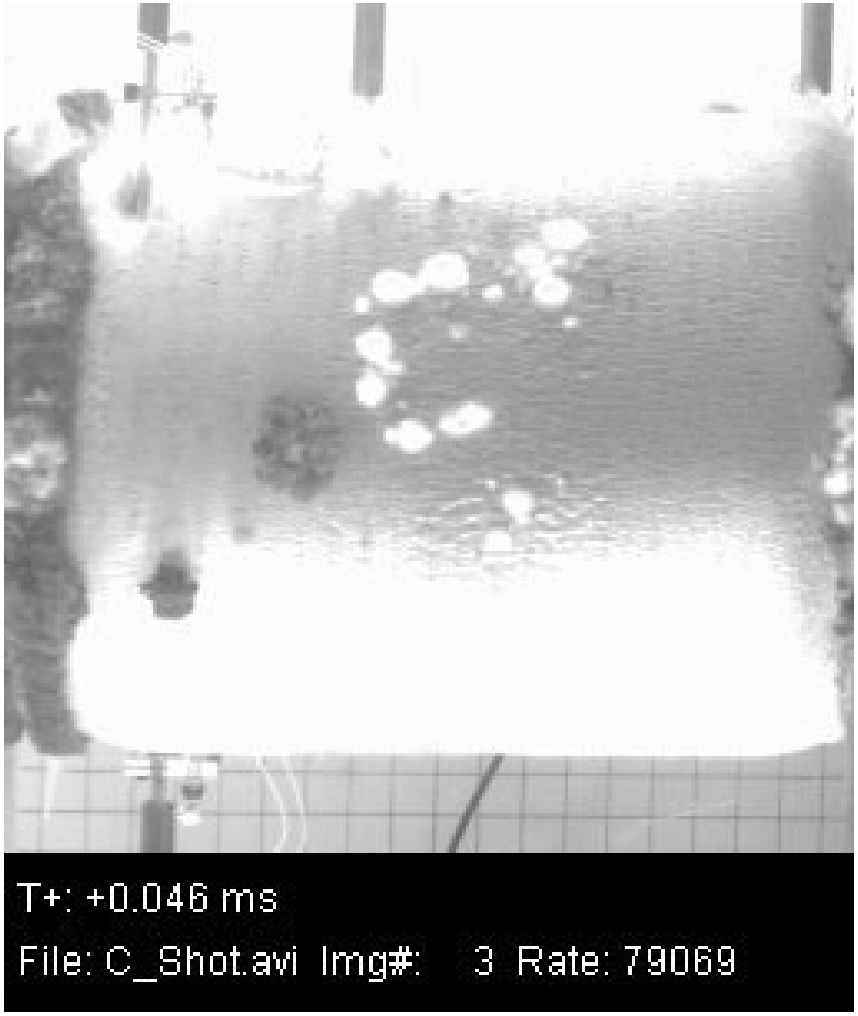

Phantom Frame 5 – Phantom time 58 µs. The armature has expanded by more than 3X at this time and is beginning to fail in many points, but the difference between the predicted and un-predicted blow-outs remains. The places where the armature is failing due to over-expansion, look more like our predicted ruptures.

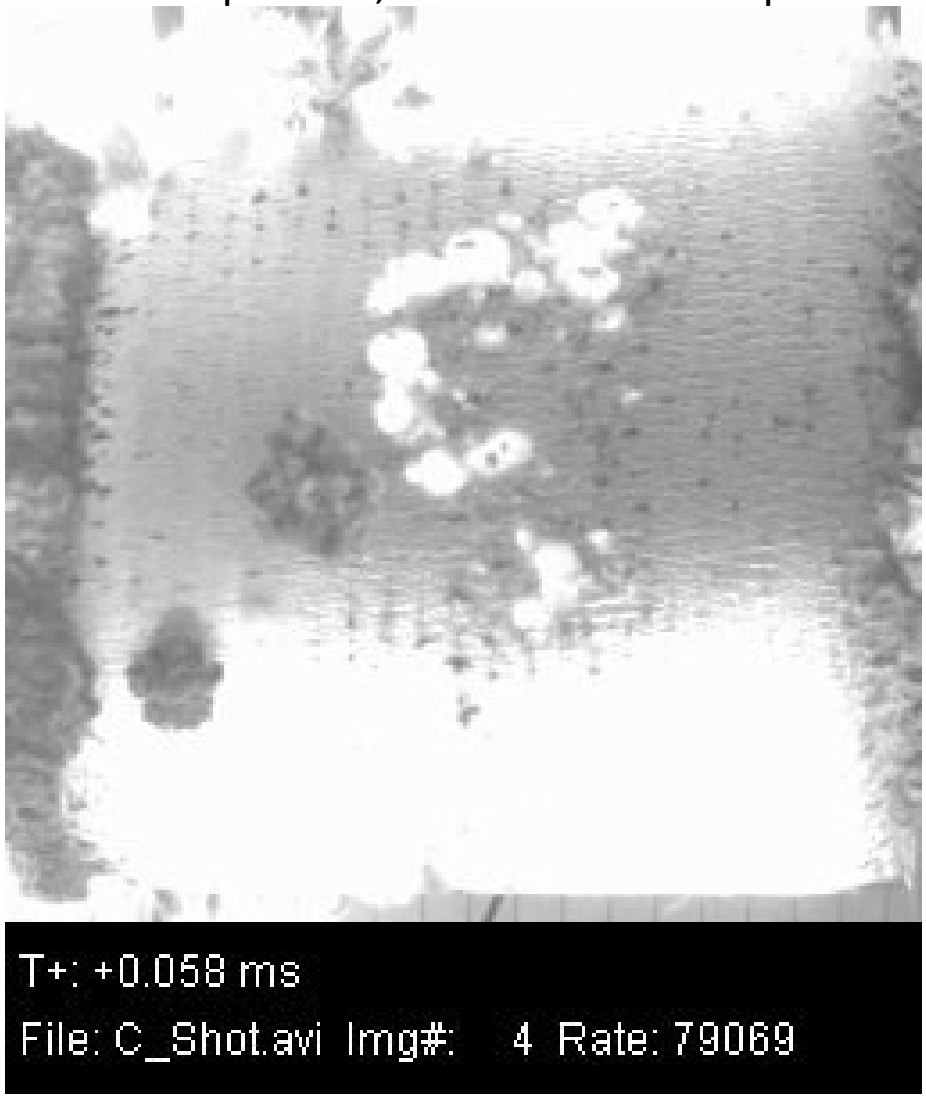

Conclusions from Camera Data

- Armature is smooth enough w/o smoother
- Bubbles cause armature to rupture in locations where they were observed.
- A set of ruptures occurred that were not predicted from pre shot inspection.
- A further understanding of the currently un-predicted ruptures is required to use the remaining two armatures in FCG tests.
- There are 23 bright ridges on the armature, indicating that they are over the shock wave interaction region rather than over the pellets.
  - They are less noticeable in the Cooke images than in the Phantom image. It also looks like the difference in top and bottom lighting causes the bands to shift from the top half to the bottom half of the cylinder. This isn't too noticeable in the Phantom image, largely because the top and bottom of the cylinder are saturated.